

Baryon scattering at high energies: wave function, impact factor, and gluon radiation

J. Bartels^{1,a}, L. Motyka^{1,2,b}

¹ II Institute for Theoretical Physics, University of Hamburg, Luruper Chaussee 149, 22761 Hamburg, Germany

² Institute of Physics, Jagellonian University, Reymonta 4, 30-059 Kraków, Poland

Received: 7 December 2007 /

Published online: 3 April 2008 – © Springer-Verlag / Società Italiana di Fisica 2008

Abstract. The scattering of a baryon consisting of three massive quarks is investigated in the high energy limit of perturbative QCD. A model of a relativistic proton-like wave function, dependent on valence quark longitudinal and transverse momenta and on quark helicities, is proposed, and we derive the baryon impact factors for two, three and four t -channel gluons. We find that the baryonic impact factor can be written as a sum of three pieces: in the first one a subsystem consisting of two of the three quarks behaves very much like the quark–antiquark pair in γ^* scattering, whereas the third quark acts as a spectator. The second term belongs to the odderon, whereas in the third (C -even) piece all three quarks participate in the scattering. This term is new and has no analogue in γ^* scattering. We also study the small x evolution of gluon radiation for each of these three terms. The first term follows the same pattern of gluon radiation as the γ^* -initiated quark–antiquark dipole, and, in particular, it contains the BFKL evolution followed by the $2 \rightarrow 4$ transition vertex (triple pomeron vertex). The odderon term is described by the standard BKP evolution, and the baryon couples to both known odderon solutions, the Janik–Wosiek solution and the BLV solution. Finally, the t -channel evolution of the third term starts with a three-reggeized gluon state, which then, via a new $3 \rightarrow 4$ transition vertex, couples to the four-gluon (two-pomeron) state. We briefly discuss a few consequences of these findings, in particular the pattern of unitarization of high energy baryon scattering amplitudes.

1 Introduction

In recent years deep inelastic electron proton or electron nucleus scattering (DIS) at small x has attracted much interest, and it has stimulated intense studies of high energy QCD. At high energies, the total cross section of a virtual photon scattering on a target, in a first approximation, can be described in terms of a photon impact factor and a Balitsky–Fadin–Kuraev–Lipatov (BFKL) Green’s function [1–12]. When restricting to the large N_c limit, and assuming a large target, unitarity corrections to this first approximation are described by the non-linear Balitsky–Kovchegov (BK) equation [13–15] which, in the language of BFKL Green’s functions, represents the infinite sum of fan diagrams [16]. The BK equation was initially obtained in the s -channel color dipole picture (in the large N_c limit) [17–19]. Beyond the large N_c limit one has to include the full color structure of the $2 \rightarrow 4$ reggeized gluon vertex [20], which leads to the Balitsky hierarchy of integral equations [13] or to the Jalilian-Marian–Iancu–McLerran–Weigert–Leonidov–Kovner (JIMWLK) equations [21–26]. In many of these calculations the incoming virtual photon

plays a vital rôle: its large virtuality Q^2 justifies the use of perturbation theory, and its impact factor consists of a quark–antiquark pair, which forms a color dipole configuration. This simple structure is also intimately connected with the fan-like structure of the diagrams resummed by the non-linear BK equation.

The advent of the LHC challenges us with the task of developing a theoretical understanding of scattering in high energy proton–proton collisions, which is related to the structure of unitarity corrections in baryon–baryon scattering. In this paper we will perform a study of the high energy behavior of baryon scattering within perturbative QCD. It is clear that the problem of high energy nucleon scattering is much more complex than it was in the virtual photon case. First of all, in nucleon–nucleon or nucleon–nucleus scattering the incoming projectiles are non-perturbative, and the accuracy of perturbative calculations is not under good theoretical control. We shall circumvent this problem by studying a fictitious scattering process of a heavy and small *baryonium* system, in analogy to the heavy *onium* proposed as a test case for perturbative unitarity corrections in DIS [19]. For such processes the perturbative calculations provide reliable results. Next, the baryonium scattering is expected to differ significantly from the onium scattering. The main reason

^a e-mail: bartels@mail.desy.de

^b e-mail: motyka@th.if.uj.edu.pl, motyka@mail.desy.de

is the difference of the color structure: in contrast to the color dipole the baryon is a color singlet formed by three valence quarks. Also, the application of the large N_c limit, which played the crucial rôle in the construction of the dipole model, is rather difficult in the baryon case: one needs exactly N_c quarks to build the color singlet of the $SU(N_c)$ group, and this system becomes rather complex for $N_c \rightarrow \infty$. In fact, a few years ago, it was explicitly pointed out [27] that the simple picture of gluon radiation that has emerged in the QCD dipole picture does not work in the case of an incoming three-quark color singlet system; however, no alternative solution had been derived. Thus, we shall address the issue of gluon radiation from three quarks at $N_c = 3$, within a perturbative baryonic system and compare with the perturbative quark–antiquark system.

The basic and universal object that characterizes properties of the baryon is its wave function. Inspired by the success of the concept of the *photon wave function* [17, 18], which turned out to be very fruitful in studies of high energy scattering, we start from a local three-fermion quark current operator with the quantum numbers of the proton and construct a relativistic invariant infinite momentum frame wave function for the lowest Fock component of the baryon, consisting of three valence quarks. The resulting wave function contains a non-trivial dependence on quark helicities and angular momenta. For the current operator we chose the baryonic operator proposed by Ioffe [28, 29], which has been shown to provide a reasonable phenomenological prescription of the nucleon properties [30]. In order to take into account the non-perturbative nature of the baryon we make use of the Borel transform technique that has been developed in the context of QCD sum rules.

This paper is not intended yet to deal with a detailed phenomenology of the baryon structure and scattering – thus we do not attempt, for example, to tune the obtained wave function to describe the existing data on proton form factors and high energy scattering. Nevertheless, apart from developing a theoretical laboratory for studying scattering of baryon states at high energies, one may hope that our perturbative analysis finds *structures* that remain also relevant beyond the perturbatively safe region. An extrapolation of our results on the heavy baryonium to the realistic proton case may, therefore, very well allow for some useful phenomenology. More detailed studies in this direction will be left for future work.

Starting from integrals over squares of these baryonic wave functions and coupling t -channel gluons to the three quark lines we define baryonic impact factors, in close analogy with the photon impact factor in deep inelastic electron proton scattering. The small- x evolution of baryon scattering amplitude will be analyzed, again, following the strategy developed in the context of the virtual photon scattering [20, 31, 32]. First we consider, in lowest order, the elastic scattering of the baryonic system on a single quark: by coupling two t -channel gluons to the three-quark system, the baryonic impact factor is obtained. Three or four t -channel gluons appear if one considers, again at lowest order, multi-particle amplitudes, e.g. $3 \rightarrow 3$ processes in a suitably defined high energy limit. In the next step, one

considers higher order diagrams in the leading logarithmic approximation: this leads to rapidity evolution equations, describing the radiation of gluons from the three-quark system.

Our main results are the following. We propose a model of the baryon wave function with a non-trivial quark helicity and angular momentum structure. Then we express the baryon impact factor in terms of the wave function, for an arbitrary number of coupling gluons. The obtained baryonic impact factor can be written as a sum of several pieces, each of them having its own evolution equation. First, there is a term in which one pair out of the three quarks scatters whereas the third quark acts as a spectator. Although the two quarks that participate in the interaction are in a color anti-triplet configuration, they behave very much like the quark–antiquark pair in the photon case. In the lowest order, two t -channel gluons couple to this quark pair. In higher order the two gluons start to reggeize and to produce the full BFKL ladder, while the third quark of the baryon state remains an inactive spectator. Also, the well-known $2 \rightarrow 4$ gluon vertex appears, indicating the beginning of the same fan-like structure as in the quark–antiquark case. Altogether, this piece of the baryon impact factor radiates gluons in very much the same way as the quark–antiquark pair in the photon case.

Next, there is the odderon term, similar to the one discussed in [33]: here all three quarks participate, and the t -channel state carries $C = -1$. In lowest order, three gluons couple to the three quarks; in higher order the state evolves according to the Bartels–Kwieciński–Praszałowicz (BKP) evolution equation [34–36].

Finally, a third, C -even, piece of the baryonic impact factor appears in which again all three quarks participate. This piece has no counterpart in the quark–antiquark case and, together with the odderon, it makes the baryon really behaving differently from the photon (or the vector meson). The state consists of one reggeized gluon with even signature and two usual odd reggeized gluons. It obeys the BKP evolution in the three-reggeon channel and it decays into four reggeized gluons via a new gauge invariant $3 \rightarrow 4$ reggeized gluon vertex.

The paper is organized as follows. We begin with a short section describing the general framework in which our calculations are carried out. We then (Sect. 3) turn to the baryon wave function, which enters the baryon impact factor. In the following Sect. 4 we describe the baryon impact factor and its decomposition into the three pieces described above, and in Sect. 5 we discuss the rapidity evolution of these pieces. Section 6 contains a short discussion of the baryonic impact factor in configuration space, and in Sect. 7 we analyze the quark–diquark limit of the baryon wave function. Finally, in Sect. 8 we summarize our results and discuss a few potential implications.

2 The framework

In our calculation we will follow the analysis of the scattering of a virtual photon described in [31, 32]. In leading

order the scattering of a virtual photon off a quark is described by the exchange of two gluons. The coupling to the photon is described by the photon impact factor, $D_{2,0}$, which most easily is obtained by the energy discontinuity of a closed quark loop (Fig. 1). Making use of the Regge factorization, the same impact factor can also be used in other elastic scattering processes, e.g. in the scattering of a virtual photon on a heavy onium target. Higher order corrections, in the leading logarithmic approximation, lead to the reggeization of the t -channel gluons and to the exchange of a BFKL pomeron between the photon impact factor and the target.

If one is looking for corrections containing more than two reggeized t -channel gluons one has to go beyond the leading logarithmic approximation. In the elastic scattering process $\gamma^* + q \rightarrow \gamma^* + q$, both leading order and NLO corrections retain the structure of a single ladder. A t -channel state with four reggeized gluons appears first in NNLO. A convenient way to avoid the complications connected with such a high order calculation is the study of multi-particle processes, e.g. the $3 \rightarrow 3$ process $\gamma^* + q + q \rightarrow \gamma^* + q + q$, the scattering of a virtual photon on two independent quarks (Fig. 2) in the triple Regge limit. This process depends upon three independent energy variables,

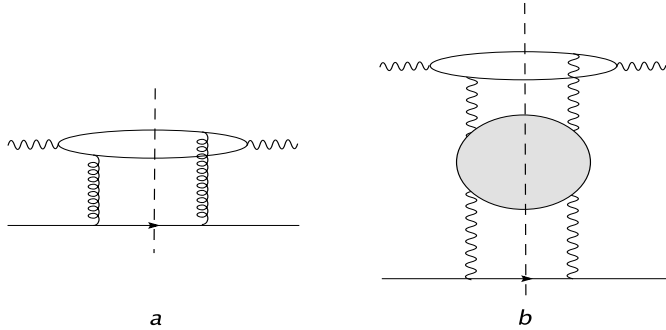


Fig. 1. Energy discontinuity of the $2 \rightarrow 2$ process: $\gamma^* + q \rightarrow \gamma^* + q$

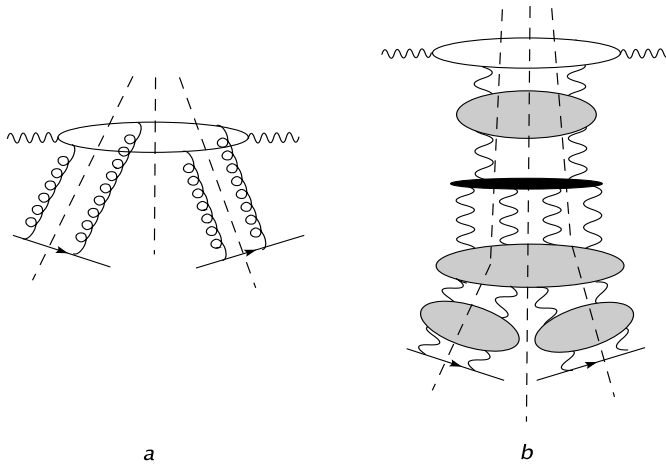


Fig. 2. Multiple energy discontinuities of the $3 \rightarrow 3$ process: $\gamma^* + q + q \rightarrow \gamma^* + q + q$: **a** lowest order diagram, **b** two examples of higher order diagrams

and the triple energy discontinuity can be easily computed in the approximation where, in each order perturbation theory, the maximal number of large energy logarithms is kept. The lowest order contribution is described by the exchange of four gluons. In higher order, these t -channel gluons reggeize and start to interact. As discussed in detail in [31, 32], the all order result can be cast into the two sets of diagrams shown in Fig. 3.

The first term starts, at the photon impact factor, with a BFKL Green's function, then undergoes the transition into the four gluons and continues with the BKP evolution of the four-gluon state. In the large- N_c limit, the four-gluon state turns into two non-interacting BFKL systems, i.e. we see the beginning of the fan-diagram structure of the BK equation. The second term consists of a simple BFKL Green's function, with higher order splittings of the reggeized gluons at the lower end. As a remarkable feature of this results, in both contributions only two reggeized gluons couple to the photon impact factor, despite the fact that diagrams with four gluons – such as the one shown in Fig. 2a – are included: the apparent ‘disappearance’ of these contributions is a result of the gluon reggeization, which manifests itself in generalized bootstrap relations.

The same strategy can be used to investigate t -channel states with higher number of t -channel reggeized gluons. For example, six gluons appear in the eight-point amplitude $\gamma^* + q + q + q \rightarrow \gamma^* + q + q + q$, i.e. the scattering of a virtual photon on three independent quarks. The analysis of this case has been investigated in [32].

Although these results are – initially – derived in the context of a higher order multi-particle processes (e.g. the $3 \rightarrow 3$ scattering process), they nevertheless can be used also in a $2 \rightarrow 2$ process. The diagrams shown in Fig. 3 satisfy reggeon unitarity equations in all three t -channels. Taking the discontinuity across the four-reggeon state, the partial wave above this can be used to construct the four-reggeon state in the $2 \rightarrow 2$ process shown in Fig. 4.

In this paper we will apply the same construction, replacing the virtual photon by a three-quark system. Modeled by the four-fermion operator introduced by Ioffe in the context of the QCD sum rules [28, 29, 37], the incom-

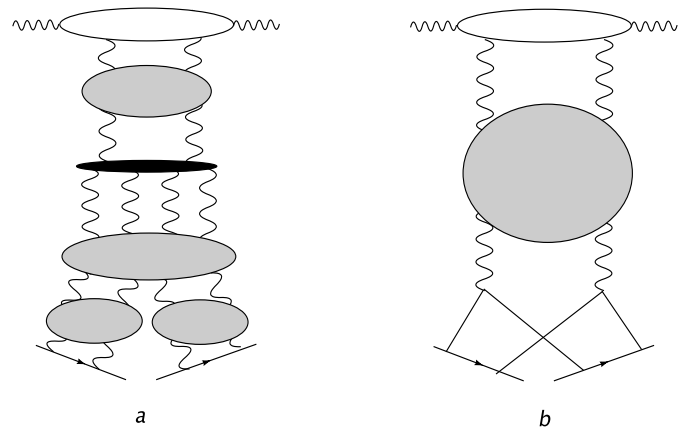


Fig. 3. Decomposition of the sum of all diagrams in Fig. 2b into **a** irreducible and **b** reggeizing pieces

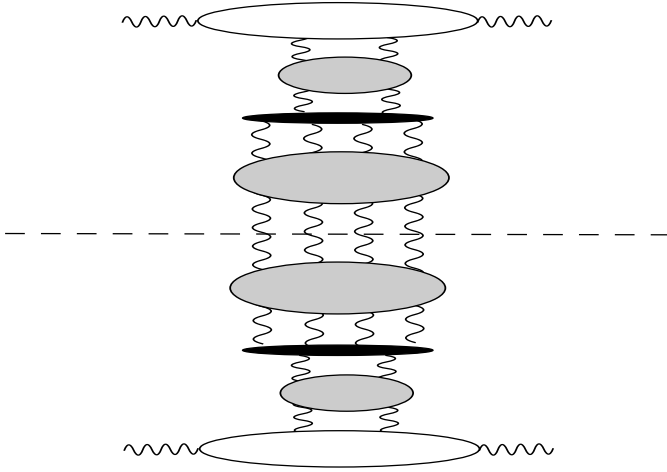


Fig. 4. Four-gluon contribution to the reggeon unitarity equation of elastic $\gamma^* \gamma^*$ scattering

ing ‘baryon’ splits into three quarks, which then couple to 2, 3, or 4 gluons. In order to take into account the non-local nature of the incoming baryonic bound state we introduce a form factor: we employ a technique used in the QCD sum rules [37] and use the Borel transform of the perturbative expression [38–40]. The exponential nature of this form factor also guarantees the convergence of the momentum integrals inside the impact factor.

3 The baryon wave function

We consider the multiple discontinuity of a non-forward baryon impact factor in elastic high energy scattering. Large momenta are directed along the z -axis, and the incoming and outgoing baryons move at small angles with respect to the z -axis, as shown in Fig. 5. Their momenta P , P' have a large “+” light-cone component, P^+ , and their transverse momenta are denoted by \mathbf{P} , \mathbf{P}' , respectively. We introduce the light-like vector $q^\mu = (q, 0, 0, -q)$, $q^2 = 0$ with $s = (P + q)^2 \simeq 2P \cdot q$, and we assume that s is large: $s \gg M^2, \mathbf{P}^2, \mathbf{P}'^2$. The quark momenta p_i are

$$p_i^\mu = (p_i^0, \mathbf{p}_i, p_i^z), \quad p_i^+ = p_i^0 + p_i^z, \quad p_i^- = p_i^0 - p_i^z. \quad (1)$$

For the longitudinal quark momenta it will sometimes be convenient to use the notation

$$p_i^+ = \alpha_i P^+, \quad p_i^- = \beta_i q^-. \quad (2)$$

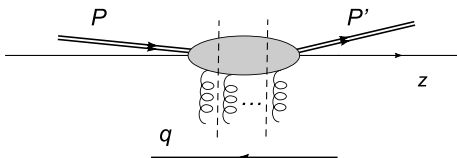


Fig. 5. Multiple discontinuity of the impact factor for elastic baryon scattering

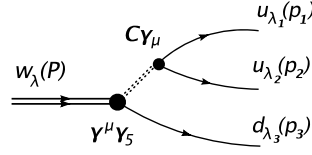


Fig. 6. The proton vertex as given by the Ioffe current

We shall use $\hat{p} = \gamma_\mu p^\mu = \gamma \cdot p$ for contraction of four-vectors and Dirac γ matrices. The adopted model of the proton state is defined by

$$\langle 0 | \eta(0) | N(P, \lambda) \rangle = A_N w_\lambda(P), \quad (3)$$

where $w_\lambda(P)$ is the proton spinor with momentum P and helicity λ ,

$$\eta(x) = \varepsilon_{\kappa_1 \kappa_2 \kappa_3} [(u^{\kappa_1}(x))^T C \gamma^\mu u^{\kappa_2}(x)] \gamma_\mu \gamma_5 d^{\kappa_3}(x) \quad (4)$$

is the baryonic Ioffe current [28, 29], C is the charge conjugation matrix, and κ_i are color indices. The Ioffe operator is not the only possible choice of the baryon current – in the context of distribution amplitudes, the possible baryonic operators for the proton were classified in [41, 42], and it was shown that the Ioffe current gives a rather good description of the baryon form factors [30]. We therefore chose, as a test case, the Ioffe operator to model the baryonic impact factor.¹

For the calculation of the baryonic impact factor we will need the matrix elements (Fig. 6) in the helicity basis,

$$[\bar{d}_{\lambda_3}(p_3) \gamma_5 \gamma_\mu w_\lambda(P)] \cdot [\bar{u}_{\lambda_1}(p_1) \gamma^\mu C \gamma^0 u_{\lambda_2}^*(p_2)]. \quad (5)$$

In the second term we can also write

$$[\bar{u}_{\lambda_1}(p_1) \gamma^\mu v_{\lambda_2}(p_2)], \quad (6)$$

where v (in the Dirac notation) denotes the v -spinor of the u quark.

3.1 The massless quark case

Using the calculus described by Brodsky and Lepage [43] we compute the Dirac spinor matrix elements. The details of the calculations are described in the appendix. For simplicity, we start from the massless quark case, and the case

¹ It is worthwhile to stress that our baryon wave functions are different from the distribution amplitudes. In the collinear approach one probes the baryon with a hard external scale Q^2 and the baryon structure is represented by series of distribution amplitudes with increasing twist, that is with increasing power-like suppression at large Q^2 . The distribution amplitudes depend on the quark longitudinal momenta, and they obey evolution equations in $\log Q^2$. In contrast to that, we are interested in the baryon wave function with full momentum dependence probed at a moderate momentum scale, and the evolution applies to the rapidity of gluons radiated from the baryon impact factor.

of massive quarks will be analyzed afterwards. Thus, we obtain

$$\begin{aligned} & \frac{[\bar{d}_\lambda(p_3)\gamma_5\gamma_\mu w_\lambda(P)] \cdot [\bar{u}_{\lambda_1}(p_1)\gamma^\mu C\gamma^0 u_{\lambda_2}^*(p_2)]}{\sqrt{\alpha_1\alpha_2\alpha_3}} \\ &= 2\lambda\delta_{-\lambda_1,\lambda_2} \left\{ \delta_{\lambda_1,\lambda} \left[\left(\frac{\mathbf{p}_2}{\alpha_2} - \mathbf{P} \right) \cdot \left(\frac{\mathbf{p}_1}{\alpha_1} - \frac{\mathbf{p}_3}{\alpha_3} \right) \right. \right. \\ & \quad \left. \left. - i\lambda \left(\frac{\mathbf{p}_2}{\alpha_2} - \mathbf{P} \right) \times \left(\frac{\mathbf{p}_1}{\alpha_1} - \frac{\mathbf{p}_3}{\alpha_3} \right) \right] \right. \\ & \quad \left. + \delta_{\lambda_2,\lambda} \left[\left(\frac{\mathbf{p}_1}{\alpha_1} - \mathbf{P} \right) \cdot \left(\frac{\mathbf{p}_2}{\alpha_2} - \frac{\mathbf{p}_3}{\alpha_3} \right) \right. \right. \\ & \quad \left. \left. - i\lambda \left(\frac{\mathbf{p}_1}{\alpha_1} - \mathbf{P} \right) \times \left(\frac{\mathbf{p}_2}{\alpha_2} - \frac{\mathbf{p}_3}{\alpha_3} \right) \right] \right\}, \end{aligned} \quad (7)$$

and,

$$\begin{aligned} & \frac{[\bar{d}_{-\lambda}(p_3)\gamma_5\gamma_\mu w_\lambda(P)] \cdot [\bar{u}_{\lambda_1}(p_1)\gamma^\mu C\gamma^0 u_{\lambda_2}^*(p_2)]}{\sqrt{\alpha_1\alpha_2\alpha_3}} \\ &= 2M\delta_{-\lambda_1,\lambda_2} \left\{ \delta_{\lambda_1,\lambda} \boldsymbol{\eta}_\lambda \cdot \left(\frac{\mathbf{p}_2}{\alpha_2} - \frac{\mathbf{p}_3}{\alpha_3} \right) \right. \\ & \quad \left. + \delta_{\lambda_2,\lambda} \boldsymbol{\eta}_\lambda \cdot \left(\frac{\mathbf{p}_1}{\alpha_1} - \frac{\mathbf{p}_3}{\alpha_3} \right) \right\}, \end{aligned} \quad (8)$$

where the transverse complex vector $\boldsymbol{\eta}_\lambda$ is defined by

$$\boldsymbol{\eta}_\lambda = (1, i\lambda), \quad \lambda = \pm 1, \quad (9)$$

and $\mathbf{P} = \mathbf{p}_1 + \mathbf{p}_2 + \mathbf{p}_3$ is the transverse momentum of the incoming baryon. The cross product of two transverse vectors $\mathbf{p}_1 = (p_1^x, p_1^y)$ and $\mathbf{p}_2 = (p_2^x, p_2^y)$ should be understood as a number, $\mathbf{p}_1 \times \mathbf{p}_2 = p_1^x p_2^y - p_1^y p_2^x$. It turns out that (7) may be re-expressed in a more compact form, by using the vectors $\boldsymbol{\eta}_\lambda$ with the following identity:

$$\begin{aligned} (\mathbf{p}_1 \cdot \boldsymbol{\eta}_\lambda)(\mathbf{p}_2 \cdot \boldsymbol{\eta}_{-\lambda}) &= (p_1^x + i\lambda p_1^y)(p_2^x - i\lambda p_2^y) \\ &= p_1^x p_2^x + p_1^y p_2^y + i\lambda(p_1^y p_2^x - p_1^x p_2^y) \\ &= \mathbf{p}_1 \cdot \mathbf{p}_2 - i\lambda \mathbf{p}_1 \times \mathbf{p}_2, \end{aligned} \quad (10)$$

which holds for any pair of transverse vectors, \mathbf{p}_1 and \mathbf{p}_2 . Using this relation one gets

$$\begin{aligned} & \frac{[\bar{d}_\lambda(p_3)\gamma_5\gamma_\mu w_\lambda(P)] \cdot [\bar{u}_{\lambda_1}(p_1)\gamma^\mu C\gamma^0 u_{\lambda_2}^*(p_2)]}{\sqrt{\alpha_1\alpha_2\alpha_3}} = \\ & 2\delta_{-\lambda_1,\lambda_2} \times \left\{ \delta_{\lambda_1,\lambda} \left[\boldsymbol{\eta}_\lambda \cdot \left(\frac{\mathbf{p}_2}{\alpha_2} - \mathbf{P} \right) \right] \left[\boldsymbol{\eta}_{-\lambda} \cdot \left(\frac{\mathbf{p}_1}{\alpha_1} - \frac{\mathbf{p}_3}{\alpha_3} \right) \right] \right. \\ & \quad \left. + \delta_{\lambda_2,\lambda} \left[\boldsymbol{\eta}_\lambda \cdot \left(\frac{\mathbf{p}_1}{\alpha_1} - \mathbf{P} \right) \right] \left[\boldsymbol{\eta}_{-\lambda} \cdot \left(\frac{\mathbf{p}_2}{\alpha_2} - \frac{\mathbf{p}_3}{\alpha_3} \right) \right] \right\}. \end{aligned} \quad (11)$$

In what follows, we shall express all formulae in this compact notation.

Next we couple a gluon of momentum $k = \beta q + \mathbf{k}$ to one of the quark lines with momentum p_i (Fig. 7). Fixing the momenta of the outgoing quarks at p_1 , p_2 , and p_3 , the quark line to the left of the gluon vertex carries momentum $p_i - k$. Using, at the gluon vertex, the eikonal approximation, one arrives at the spinorial factor \hat{q} . With $2p_i \cdot q = \alpha_i s \gg \mathbf{p}_i^2, \mathbf{k}^2$ etc., one obtains, for the upper u quark,

$$\bar{u}(p_1)\hat{q}(\hat{p}_1 - \hat{k}) = 2p_1 \cdot q \bar{u}(p_1 - k) + \dots, \quad (12)$$

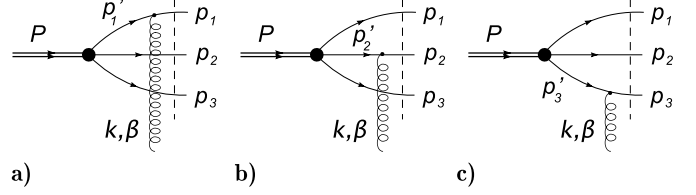


Fig. 7. Single gluon coupling to the baryon $\rightarrow X$ transition

where \dots stands for terms which are power suppressed in s . An analogous expression holds for the d quark, whereas for the second u quark we use

$$(\hat{p}_2 - \hat{k})\hat{q}u^*(p_2) = 2p_2 \cdot qu^*(p_2 - k) + \dots \quad (13)$$

As a result, on the r.h.s. of (12) and (13), the transverse momentum of the quark spinor coincides with the transverse momentum of the internal quark line next to the baryon vertex. The sum of the outgoing transverse momenta equals

$$\mathbf{p}_1 + \mathbf{p}_2 + \mathbf{p}_3 = \mathbf{P} + \mathbf{k}. \quad (14)$$

Matrix elements corresponding to multi-gluon couplings to spinor lines may be simplified by iterating (12) in the following way:

$$\begin{aligned} & \bar{u}(p)\hat{q}[\gamma \cdot (p - k_1)]\hat{q} \dots \hat{q}[\gamma \cdot (p - k_1 - \dots - k_n)] \simeq \\ & (2p \cdot q)^n \bar{u}(p - k_1 - \dots - k_n). \end{aligned} \quad (15)$$

For completeness, we recall that, in the case of an outgoing antiquark, an additional minus sign appears:

$$-(\hat{p} - \hat{k})\hat{q}v(p) = -2p \cdot qv(p - k) + \dots, \quad (16)$$

This minus sign is due to the opposite direction of the momentum along the antifermion line. Similarly,

$$\begin{aligned} & [-\gamma \cdot (p - k_1 - \dots - k_n)]\hat{q} \dots \hat{q}[-\gamma \cdot (p - k_1)]\hat{q}v(p) \simeq \\ & (-2p \cdot q)^n v(p - k_1 - \dots - k_n). \end{aligned} \quad (17)$$

This change in sign plays a crucial rôle in the photon impact factor [17, 18].

We are now ready to describe the amplitude for the process baryon + gluon \rightarrow three quarks, defined by the diagrams shown in Fig. 7. We define the shifted momentum of the upper quark

$$\mathbf{p}_1' = \mathbf{p}_1 - \mathbf{k}, \quad (18)$$

with

$$\mathbf{p}_1' + \mathbf{p}_2 + \mathbf{p}_3 = \mathbf{P}, \quad (19)$$

and use

$$p_1'^2 = \alpha_1 \left(M^2 + \mathbf{P}^2 - \frac{\mathbf{p}_1'^2}{\alpha_1} - \frac{\mathbf{p}_2^2}{\alpha_2} - \frac{\mathbf{p}_3^2}{\alpha_3} \right), \quad (20)$$

(and analogous expressions for the gluon coupling to quark lines 2 and 3). We introduce the amplitudes

$$\begin{aligned}
\Theta_{\lambda}^{(\lambda_1, \lambda_2) \lambda}(\{\alpha_i\}, \{\mathbf{p}_1, \mathbf{p}_2, \mathbf{p}_3\}; \mathbf{P}) = & \\
& \lambda \mathcal{N}_{\Theta} \frac{2\sqrt{\alpha_1 \alpha_2 \alpha_3}}{M^2 + \mathbf{P}^2 - \frac{\mathbf{p}_1^2}{\alpha_1} - \frac{\mathbf{p}_2^2}{\alpha_2} - \frac{\mathbf{p}_3^2}{\alpha_3}} \\
& \times \delta_{-\lambda_1, \lambda_2} \delta^{(2)}(\mathbf{p}_1 + \mathbf{p}_2 + \mathbf{p}_3 - \mathbf{P}) \\
& \times \left\{ \delta_{\lambda_1, \lambda} \left[\boldsymbol{\eta}_{\lambda} \cdot \left(\frac{\mathbf{p}_2}{\alpha_2} - \mathbf{P} \right) \right] \left[\boldsymbol{\eta}_{-\lambda} \cdot \left(\frac{\mathbf{p}_1}{\alpha_1} - \frac{\mathbf{p}_3}{\alpha_3} \right) \right] \right. \\
& \left. + \delta_{\lambda_2, \lambda} \left[\boldsymbol{\eta}_{\lambda} \cdot \left(\frac{\mathbf{p}_1}{\alpha_1} - \mathbf{P} \right) \right] \left[\boldsymbol{\eta}_{-\lambda} \cdot \left(\frac{\mathbf{p}_2}{\alpha_2} - \frac{\mathbf{p}_3}{\alpha_3} \right) \right] \right\}, \quad (21) \\
\Theta_{\lambda}^{(\lambda_1, \lambda_2) - \lambda}(\{\alpha_i\}, \{\mathbf{p}_1, \mathbf{p}_2, \mathbf{p}_3\}; \mathbf{P}) = & \\
& \mathcal{N}_{\Theta} \frac{2M\sqrt{\alpha_1 \alpha_2 \alpha_3}}{M^2 + \mathbf{P}^2 - \frac{\mathbf{p}_1^2}{\alpha_1} - \frac{\mathbf{p}_2^2}{\alpha_2} - \frac{\mathbf{p}_3^2}{\alpha_3}} \\
& \times \delta_{-\lambda_1, \lambda_2} \delta^{(2)}(\mathbf{p}_1 + \mathbf{p}_2 + \mathbf{p}_3 - \mathbf{P}) \\
& \times \left\{ \delta_{\lambda_1, \lambda} \boldsymbol{\eta}_{\lambda} \cdot \left(\frac{\mathbf{p}_2}{\alpha_2} - \frac{\mathbf{p}_3}{\alpha_3} \right) + \delta_{\lambda_2, \lambda} \boldsymbol{\eta}_{\lambda} \cdot \left(\frac{\mathbf{p}_1}{\alpha_1} - \frac{\mathbf{p}_3}{\alpha_3} \right) \right\}. \quad (22)
\end{aligned}$$

Here the upper three indices of Θ denote the helicities of the upper two u quarks with momenta \mathbf{p}_1 and \mathbf{p}_2 , and the lower d quark with momentum \mathbf{p}_3 , respectively. The subscript refers to the helicity λ of the incoming baryon. We leave the normalization constant \mathcal{N}_{Θ} unspecified here; the normalization will be fixed at the level of baryon wave function. The amplitudes for the diagrams shown in Fig. 7a–c are then simply obtained from (21) and (22) by the replacements $\mathbf{p}_1 \rightarrow \mathbf{p}'_1$, $\mathbf{p}_2 \rightarrow \mathbf{p}'_2$ and $\mathbf{p}_3 \rightarrow \mathbf{p}'_3$, respectively.²

Note that, for each of the three diagrams, the denominator is just the energy denominator in non-covariant perturbation theory, for instance one obtains for Fig. 7a,

$$E_{\text{baryon}} - E_{3 \text{ quark}} = \frac{1}{P^+} \left(M^2 + \mathbf{P}^2 - \frac{\mathbf{p}_1'^2}{\alpha_1} - \frac{\mathbf{p}_2'^2}{\alpha_2} - \frac{\mathbf{p}_3'^2}{\alpha_3} \right). \quad (23)$$

The amplitudes should be invariant under Lorentz boosts in the transverse directions, parametrized by a four-velocity $u^\mu \simeq (1, \mathbf{u}, 0)$, $|\mathbf{u}| \ll 1$:

$$\mathbf{p}_i \rightarrow \mathbf{p}'_i \simeq \mathbf{p}_i + \frac{1}{2} p_i^+ \mathbf{u}, \quad p_i^+ \rightarrow p_i'^+ \simeq p_i^+. \quad (24)$$

The numerators are manifestly invariant under these transformations, and the denominators may be also rewritten in an explicitly invariant form using the identity

$$\begin{aligned}
-\mathbf{P}^2 + \frac{\mathbf{p}_1^2}{\alpha_1} + \frac{\mathbf{p}_2^2}{\alpha_2} + \frac{\mathbf{p}_3^2}{\alpha_3} = & \alpha_1 \alpha_2 \left(\frac{\mathbf{p}_1}{\alpha_1} - \frac{\mathbf{p}_2}{\alpha_2} \right)^2 \\
& + \alpha_1 \alpha_3 \left(\frac{\mathbf{p}_3}{\alpha_3} - \frac{\mathbf{p}_1}{\alpha_1} \right)^2 + \alpha_2 \alpha_3 \left(\frac{\mathbf{p}_2}{\alpha_2} - \frac{\mathbf{p}_3}{\alpha_3} \right)^2, \quad (25)
\end{aligned}$$

² To be precise, the functions Θ give the *momentum dependent part* of the scattering amplitudes, up to a global normalization factor that is proportional to the strong coupling constant g . Obviously, the color factors are not accounted for in (21) and (22) – they will be treated explicitly later on.

$$\begin{aligned}
-\mathbf{P}^2 + \frac{\mathbf{p}_1^2}{\alpha_1} + \frac{\mathbf{p}_2^2}{\alpha_2} + \frac{\mathbf{p}_3^2}{\alpha_3} = & \frac{(\mathbf{p}_1 - \alpha_1 \mathbf{P})^2}{\alpha_1} + \frac{(\mathbf{p}_2 - \alpha_2 \mathbf{P})^2}{\alpha_2} \\
& + \frac{(\mathbf{p}_3 - \alpha_3 \mathbf{P})^2}{\alpha_3}. \quad (26)
\end{aligned}$$

The denominators have poles for the invariant mass of the three-quark system equal to the proton transverse mass. Clearly, this is a consequence of using a point-like vertex for the proton–quark coupling and neglecting the bound state effects. These effects cannot be described within perturbative QCD and should be modeled. Following [37–39] we propose a model that preserves Lorentz and helicity structures of the perturbative expressions, where the bound state effects are absorbed into the Borel transform.

The Borel transform of a function $f(s)$ is defined in the standard way:

$$\begin{aligned}
\mathcal{B}_s[f](M_B^2) = \lim_{n \rightarrow \infty} \frac{s^{n+1}}{n!} \left(-\frac{d}{ds} \right)^n f(s), \quad s \rightarrow \infty, \\
s/n \rightarrow M_B^2, \quad (27)
\end{aligned}$$

where M_B is the Borel parameter. In order to model the baryon scattering amplitude we shall apply two independent Borel transforms with respect to the negative virtualities $Q^2 = -P^2$ of the incoming and $Q'^2 = -P'^2$ of the outgoing baryon, to the perturbative amplitudes obtained with the point-like vertex. Equations (21) and (22) were presented for $P^2 = M^2$. The corresponding formulae for general virtualities are obtained by substitutions $M^2 \rightarrow P^2$ in the denominators. In the baryon impact factor, the virtuality P^2 appears only in the energy denominator of the vertex amplitude $\Theta_{\lambda}^{(\lambda_1, \lambda_2) \lambda_3}(\{\alpha_i\}, \{\mathbf{p}_i\}; \mathbf{P})$ of the incoming baryon, and the virtuality P'^2 only in the denominator of the amplitude $[\Theta_{\lambda}^{(\lambda_1, \lambda_2) \lambda_3}(\{\alpha_i\}, \{\mathbf{p}_i\}; \mathbf{P}')]^*$ of the outgoing state (see Sect. 4 for more details). Therefore the two Borel transforms may be performed independently for each Θ , that is already at the level of the baryon wave function. Thus we evaluate

$$\mathcal{B}_{Q^2} \left[\frac{1}{Q^2 + M_X^2} \right] (M_B^2) = \exp(-M_X^2/M_B^2). \quad (28)$$

This result, applied to the amplitudes Θ , leads to the substitution

$$\frac{1}{P^2 + \mathbf{P}^2 - \sum_{i=1}^3 \frac{\mathbf{p}_i^2}{\alpha_i}} \rightarrow -\exp \left[-\frac{1}{M_B^2} \left(\sum_{i=1}^3 \frac{\mathbf{p}_i^2}{\alpha_i} - \mathbf{P}^2 \right) \right]. \quad (29)$$

Before we complete the model we shall perform some simplifications. We shall absorb into the wave functions a phase space factor $(\alpha_1 \alpha_2 \alpha_3)^{-1}$ that appears in the baryon impact factor as a result of on-mass-shell conditions of the cut quark lines. In this way, the factor $\sqrt{\alpha_1 \alpha_2 \alpha_3}$ present in the amplitudes Θ will be removed from the

wave functions. Obviously, the integration measure will be suitably modified as well. For simplicity, we introduce a normalization constant, \mathcal{N} , of the wave function, which will be fixed later. Thus, we choose the natural value of the Borel parameter $M_B = M$ and obtain a model of the baryon wave function,

$$\begin{aligned} \Psi_\lambda^{(\lambda_1, \lambda_2)\lambda}(\{\alpha_i\}, \{\mathbf{p}_i\}; \mathbf{P}) &= \lambda \mathcal{N} e^{-\frac{1}{M^2}(-\mathbf{P}^2 + \frac{\mathbf{p}_1^2}{\alpha_1} + \frac{\mathbf{p}_2^2}{\alpha_2} + \frac{\mathbf{p}_3^2}{\alpha_3})} \\ &\times \delta_{-\lambda_1, \lambda_2} \delta^{(2)}(\mathbf{p}_1 + \mathbf{p}_2 + \mathbf{p}_3 - \mathbf{P}) \\ &\times \left\{ \delta_{\lambda_1, \lambda} \left[\boldsymbol{\eta}_\lambda \cdot \left(\frac{\mathbf{p}_2}{\alpha_2} - \mathbf{P} \right) \right] \left[\boldsymbol{\eta}_{-\lambda} \cdot \left(\frac{\mathbf{p}_1}{\alpha_1} - \frac{\mathbf{p}_3}{\alpha_3} \right) \right] \right. \\ &\left. + \delta_{\lambda_2, \lambda} \left[\boldsymbol{\eta}_\lambda \cdot \left(\frac{\mathbf{p}_1}{\alpha_1} - \mathbf{P} \right) \right] \left[\boldsymbol{\eta}_{-\lambda} \cdot \left(\frac{\mathbf{p}_2}{\alpha_2} - \frac{\mathbf{p}_3}{\alpha_3} \right) \right] \right\}, \quad (30) \\ \Psi_\lambda^{(\lambda_1, \lambda_2)-\lambda}(\{\alpha_i\}, \{\mathbf{p}_i\}; \mathbf{P}) &= \mathcal{N} e^{-\frac{1}{M^2}(-\mathbf{P}^2 + \frac{\mathbf{p}_1^2}{\alpha_1} + \frac{\mathbf{p}_2^2}{\alpha_2} + \frac{\mathbf{p}_3^2}{\alpha_3})} \\ &\times \delta_{-\lambda_1, \lambda_2} \delta^{(2)}(\mathbf{p}_1 + \mathbf{p}_2 + \mathbf{p}_3 - \mathbf{P}) \\ &\times M \left\{ \delta_{\lambda_1, \lambda} \boldsymbol{\eta}_\lambda \cdot \left(\frac{\mathbf{p}_2}{\alpha_2} - \frac{\mathbf{p}_3}{\alpha_3} \right) + \delta_{\lambda_2, \lambda} \boldsymbol{\eta}_\lambda \cdot \left(\frac{\mathbf{p}_1}{\alpha_1} - \frac{\mathbf{p}_3}{\alpha_3} \right) \right\}. \quad (31) \end{aligned}$$

Clearly, the functions Ψ given by (30) and (31) are symmetric under the interchange of the u quarks, labeled by 1 and 2. When combined with the anti-symmetry in the color degrees of freedom, it implies that the full wave function is anti-symmetric under interchange of the u quarks, as it must be. Interestingly enough, a similar Gaussian form of the wave function was proposed long ago [44], and it was shown to provide a good description of the nucleon form factor data [45, 46]. An important difference with our model, however, is the presence of angular momenta of the quarks. The baryon angular momentum structure following from the model is most transparent in the coordinate representation and will be discussed in Sect. 6.

The above derivation of the baryon wave function is based on perturbative QCD methods combined with the Borel transform technique. Clearly, we are not able to control the accuracy of this procedure for the proton, as it is a genuine non-perturbative object. Therefore the obtained wave functions can only be considered as a theoretically inspired model of the proton wave function. Therefore, in the next part we give the formulae for the wave function of a baryon consisting of three quarks with the same mass m , coming in two different flavors. These formulae will permit one to consider the fictitious case of a large quark mass, for which the baryon becomes heavy and small, and the perturbative computation of its wave function and scattering is formally justified.

3.2 Massive quarks

We now apply the procedure described in the previous section to the case of the massive quarks. We skip the details of the derivation and present the result for the helicity amplitudes Θ of the transition of baryons to quarks, in which all three quarks were assumed to have the

mass m :

$$\begin{aligned} \Theta_\lambda^{(\lambda_1, \lambda_2)\lambda_3}(\{\alpha_i\}, \{\mathbf{p}_i\}; \mathbf{P}) &= \\ \mathcal{N}_\Theta \frac{2\sqrt{\alpha_1 \alpha_2 \alpha_3}}{M^2 + \mathbf{P}^2 - \frac{\mathbf{p}_1^2 + m^2}{\alpha_1} - \frac{\mathbf{p}_2^2 + m^2}{\alpha_2} - \frac{\mathbf{p}_3^2 + m^2}{\alpha_3}} \\ &\times \delta^{(2)}(\mathbf{p}_1 + \mathbf{p}_2 + \mathbf{p}_3 - \mathbf{P}) \\ &\times \left\{ \delta_{\lambda, \lambda_1} \delta_{\lambda, \lambda_2} \delta_{\lambda, \lambda_3} m \frac{\alpha_1 + \alpha_2}{\alpha_1 \alpha_2} \left(\frac{\mathbf{p}_3}{\alpha_3} - \frac{\mathbf{p}_1 + \mathbf{p}_2}{\alpha_1 + \alpha_2} \right) \cdot \boldsymbol{\eta}_{-\lambda} \right. \\ &+ \lambda \delta_{\lambda, \lambda_1} \delta_{\lambda, \lambda_2} \delta_{\lambda, -\lambda_3} m \frac{\alpha_1 + \alpha_2}{\alpha_1 \alpha_2} \left(M - \frac{m}{\alpha_3} \right) \\ &+ \delta_{\lambda, -\lambda_1} \delta_{\lambda, -\lambda_2} \delta_{\lambda, \lambda_3} m \frac{\alpha_1 + \alpha_2}{\alpha_1 \alpha_2} \left(\frac{\mathbf{p}_1 + \mathbf{p}_2}{\alpha_1 + \alpha_2} - \mathbf{P} \right) \cdot \boldsymbol{\eta}_\lambda \\ &+ \lambda \delta_{\lambda, \lambda_1} \delta_{\lambda, -\lambda_2} \delta_{\lambda, \lambda_3} \left[\left(\frac{\mathbf{p}_2}{\alpha_2} - \mathbf{P} \right) \cdot \boldsymbol{\eta}_\lambda \left(\frac{\mathbf{p}_1}{\alpha_1} - \frac{\mathbf{p}_3}{\alpha_3} \right) \cdot \boldsymbol{\eta}_{-\lambda} \right. \\ &\left. + m \left(\frac{M}{\alpha_3} - \frac{m}{\alpha_1 \alpha_2} \right) \right] \\ &+ \lambda \delta_{\lambda, -\lambda_1} \delta_{\lambda, \lambda_2} \delta_{\lambda, \lambda_3} \left[\left(\frac{\mathbf{p}_1}{\alpha_1} - \mathbf{P} \right) \cdot \boldsymbol{\eta}_\lambda \left(\frac{\mathbf{p}_2}{\alpha_2} - \frac{\mathbf{p}_3}{\alpha_3} \right) \cdot \boldsymbol{\eta}_{-\lambda} \right. \\ &\left. + m \left(\frac{M}{\alpha_3} - \frac{m}{\alpha_1 \alpha_2} \right) \right] \\ &+ \delta_{\lambda, \lambda_1} \delta_{\lambda, -\lambda_2} \delta_{\lambda, -\lambda_3} \left[M \left(\frac{\mathbf{p}_2}{\alpha_2} - \frac{\mathbf{p}_3}{\alpha_3} \right) \cdot \boldsymbol{\eta}_\lambda \right. \\ &+ m \frac{1 - \alpha_3}{\alpha_3} \left(\frac{\mathbf{p}_2}{\alpha_2} - \frac{\mathbf{p}_1 + \mathbf{p}_2}{\alpha_1 + \alpha_2} \right) \cdot \boldsymbol{\eta}_\lambda \left. \right] \\ &+ \delta_{\lambda, -\lambda_1} \delta_{\lambda, \lambda_2} \delta_{\lambda, -\lambda_3} \left[M \left(\frac{\mathbf{p}_1}{\alpha_1} - \frac{\mathbf{p}_3}{\alpha_3} \right) \cdot \boldsymbol{\eta}_\lambda \right. \\ &\left. + m \frac{1 - \alpha_3}{\alpha_3} \left(\frac{\mathbf{p}_1}{\alpha_1} - \frac{\mathbf{p}_1 + \mathbf{p}_2}{\alpha_1 + \alpha_2} \right) \cdot \boldsymbol{\eta}_\lambda \right] \left. \right\}. \quad (32) \end{aligned}$$

Note that using (10) and taking $m \rightarrow 0$ one easily recovers (21) and (22). The above formulae are promoted to the baryon wave functions Ψ , by going through the same steps as in the massless case, i.e. using the Borel transform and absorbing the α factors into the phase space factor. The final expressions for the wave functions are obtained from (32) by the replacement that combines both steps:

$$\begin{aligned} \mathcal{N}_\Theta \frac{2\sqrt{\alpha_1 \alpha_2 \alpha_3}}{M^2 + \mathbf{P}^2 - \sum_{i=1}^3 \frac{\mathbf{p}_i^2 + m^2}{\alpha_i}} &\longrightarrow \\ \mathcal{N} \exp \left[-\frac{1}{M^2} \left(\sum_{i=1}^3 \frac{\mathbf{p}_i^2 + m^2}{\alpha_i} - \mathbf{P}^2 \right) \right] & \quad (33) \end{aligned}$$

4 Baryon impact factors

4.1 General structure

The amplitudes Ψ may be combined with their complex conjugates to obtain the baryon impact factor. For the case of two gluons coupled to lines 3 and 1 we illustrate one example in Fig. 8. It was shown in the previous section that,

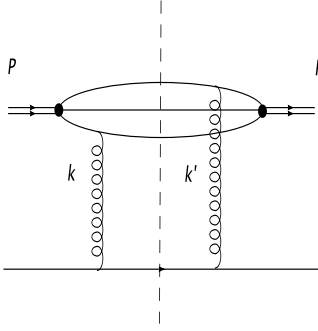


Fig. 8. A contribution to the two-gluon exchange in baryon-quark scattering

in the high energy limit the spinorial part of the multiple discontinuity can be expressed in terms of universal matrix elements given by (7) and (8), where the momenta of the quarks are evaluated at the quark-proton vertex. Also the denominator is determined by the virtuality of the quark to which the first gluon couples, and the virtuality can be expressed in terms of the momenta of the quarks at the proton vertex. Thus, the impact factor can be obtained from overlap integrals, i.e. products of wave functions with suitably adjusted momenta. As an example, we specify the overlap function corresponding to Fig. 8:

$$\begin{aligned} \mathcal{F}^{\lambda\lambda'}(\{\mathbf{k}, \mathbf{k}'\}; \mathbf{P}, \mathbf{P}') &= \sum_{\lambda_1, \lambda_2, \lambda_3} \int [d^2\mathbf{p}_i] [d\alpha_i] \\ &\times [\Psi_{\lambda'}^{(\lambda_1, \lambda_2)\lambda_3}(\{\alpha_i\}, \{\mathbf{p}_1', \mathbf{p}_2, \mathbf{p}_3\}; \mathbf{P}')]^* \\ &\times \Psi_{\lambda}^{(\lambda_1, \lambda_2)\lambda_3}(\{\alpha_i\}, \{\mathbf{p}_1, \mathbf{p}_2, \mathbf{p}_3'\}; \mathbf{P}), \end{aligned} \quad (34)$$

with the integration measure

$$\begin{aligned} [d^2\mathbf{p}_i] &= d^2\mathbf{p}_1 d^2\mathbf{p}_2 d^2\mathbf{p}_3, \\ [d\alpha_i] &= d\alpha_1 d\alpha_2 d\alpha_3 \delta(\alpha_1 + \alpha_2 + \alpha_3 - 1). \end{aligned} \quad (35)$$

In the overlap functions $\mathcal{F}^{\lambda\lambda'}$, the upper helicity labels refer to the incoming and outgoing baryon states, respectively. Analogous overlap functions are defined for the other gluon couplings, and for the full impact factor we will have to sum over all diagrams. When evaluating the sum over the intermediate helicities λ_1 , λ_2 , and λ_3 and summing over all diagrams, one finds, for the forward direction $\mathbf{P} = \mathbf{P}' = 0$, helicity conservation, i.e. the impact factor vanishes for $\lambda = -\lambda'$.

Before including the remaining energy integrals and the color factors we generalize to the case of 3 and 4 t -channel gluons. As outlined in Sect. 2, we have to consider multiple energy discontinuities. An example is shown in Fig. 9. For one of the discontinuity lines (in the case of Fig. 9, the central line) we fix the intermediate quark momenta and denote them by $\mathbf{p}_1, \mathbf{p}_2, \mathbf{p}_3$. The corresponding overlap function (Fig. 10) takes the form

$$\begin{aligned} \mathcal{F}^{\lambda\lambda'}(\{\mathbf{k}_i, \mathbf{k}'_j\}; \mathbf{P}, \mathbf{P}') &= \sum_{\lambda_1, \lambda_2, \lambda_3} \int [d^2\mathbf{p}_i] [d\alpha_i] \\ &\times [\Psi_{\lambda'}^{(\lambda_1, \lambda_2)\lambda_3}(\{\alpha_i\}, \{\mathbf{p}_1 + \mathbf{k}'_1, \mathbf{p}_2 + \mathbf{k}'_2, \mathbf{p}_3 + \mathbf{k}'_3\}; \mathbf{P}')]^* \\ &\times \Psi_{\lambda}^{(\lambda_1, \lambda_2)\lambda_3}(\{\alpha_i\}, \{\mathbf{p}_1 - \mathbf{k}_1, \mathbf{p}_2 - \mathbf{k}_2, \mathbf{p}_3 - \mathbf{k}_3\}; \mathbf{P}), \end{aligned} \quad (36)$$

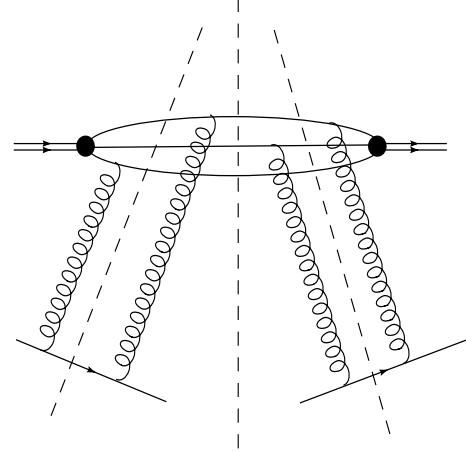


Fig. 9. A contribution to the four-gluon exchange in the scattering of a baryon on two independent quarks

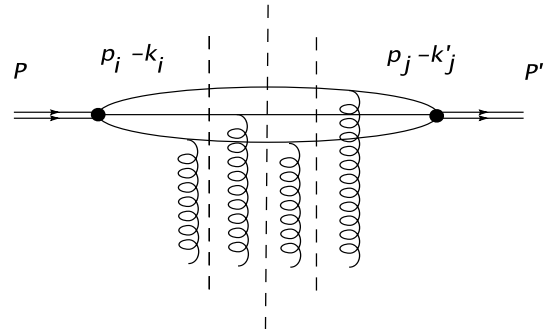


Fig. 10. Example of a diagram defining the overlap function for a multiple discontinuity in Fig. 9

where \mathbf{k}_i (\mathbf{k}'_j) is the sum of momenta delivered by the gluons to the quark line i to the left (right) of the central cutting line. Obviously,

$$\sum_i \mathbf{k}_i + \sum_j \mathbf{k}'_j = \mathbf{P}' - \mathbf{P}. \quad (37)$$

Since, as a consequence of the exponential form factor, all transverse momentum integrals are finite, we are allowed to shift, for each diagram separately, the loop momenta, such that to the right of the incoming baryon vertex the momenta become \mathbf{p}_1 , \mathbf{p}_2 , and \mathbf{p}_3 . At the outgoing baryon vertex the momenta are $\mathbf{p}_1 + \mathbf{l}_1$, $\mathbf{p}_2 + \mathbf{l}_2$, and $\mathbf{p}_3 + \mathbf{l}_3$, where \mathbf{l}_i is the sum of transverse momenta of *all* gluons coupled to the quark line i (Fig. 10):

$$\mathbf{l}_i = \sum_{j \in L_i} (\mathbf{k}_j + \mathbf{k}'_j). \quad (38)$$

In the general case the overlap function can be written as

$$\begin{aligned} \mathcal{F}^{\lambda\lambda'}(\{\mathbf{l}_i\}; \mathbf{P}, \mathbf{P}') &= \sum_{\lambda_1, \lambda_2, \lambda_3} \int [d^2\mathbf{p}_i] [d\alpha_i] \\ &\times [\Psi_{\lambda'}^{(\lambda_1, \lambda_2)\lambda_3}(\{\alpha_i\}, \{\mathbf{p}_i + \mathbf{l}_i\}; \mathbf{P}')]^* \\ &\times \Psi_{\lambda}^{(\lambda_1, \lambda_2)\lambda_3}(\{\alpha_i\}, \{\mathbf{p}_i\}; \mathbf{P}). \end{aligned} \quad (39)$$

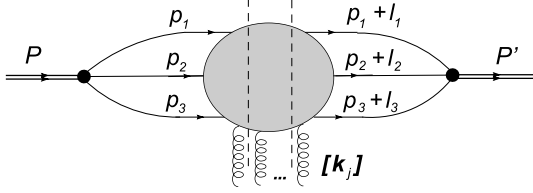


Fig. 11. Baryon impact factor

We now complete the definition of the baryonic impact factor (see Fig. 11). The general impact factor $\mathcal{I}_{AB}^{(N)}$ for the transition $A \rightarrow B$, with N gluons being coupled in the eikonal approximation, is defined as

$$\mathcal{I}_{AB}^{(N)} = \int \frac{d\beta_1}{2\pi} \frac{d\beta_2}{2\pi} \dots \frac{d\beta_{N-1}}{2\pi} \frac{q_{\mu_1} q_{\mu_2} \dots q_{\mu_N}}{s} \times \text{Disc}_{N-1} \mathcal{S}_{AB}^{\mu_1 \mu_2 \dots \mu_N}, \quad (40)$$

where $\mathcal{S}_{AB}^{\mu_1 \mu_2 \dots \mu_N}$ represents the amputated transition amplitude. In particular, for the elastic scattering of a single quark inside the baryon one obtains

$$\mathcal{I}_{qq}^{(N)} = \frac{1}{N_c} \text{Tr}[t^{a_N} t^{a_{N-1}} \dots t^{a_1}] I_{qq}^{(N)}, \quad (41)$$

where

$$I_{qq}^{(N)} = (-ig)^N. \quad (42)$$

The baryon impact factor for N t -channel gluons is then given by

$$\mathcal{B}_N^{\lambda\lambda'}(\{\mathbf{l}_i\}; \mathbf{P}, \mathbf{P}') = I_{qq}^{(N)} \sum_{\text{diagrams}} \mathcal{F}^{\lambda\lambda'}(\{\mathbf{l}_i\}; \mathbf{P}, \mathbf{P}') \mathcal{C}_N(\text{diagram}), \quad (43)$$

where the color factor reads

$$\mathcal{C}_N(\text{diagram}) = \frac{\varepsilon^{\kappa'_1 \kappa'_2 \kappa'_3} \varepsilon^{\kappa_1 \kappa_2 \kappa_3}}{3!} [t^{a_l} t^{a_{l-1}} \dots t^{a_1}]_{\kappa'_1 \kappa_1} \times [t^{b_m} t^{b_{m-1}} \dots t^{b_1}]_{\kappa'_2 \kappa_2} [t^{c_n} t^{c_{n-1}} \dots t^{c_1}]_{\kappa'_3 \kappa_3}. \quad (44)$$

In (43) the sum extends over all diagrams, and the numbers l , m and n of gluons, that couple to quark lines 1, 2 and 3, take all possible values between 1 and N with the constraint $l + m + n = N$. The overlap function $\mathcal{F}^{\lambda\lambda'}(\{\mathbf{l}_i\}; \mathbf{P}, \mathbf{P}')$ is evaluated for each diagram separately, and in each case it contains a global delta function of the transverse momenta:

$$\mathcal{F}^{\lambda\lambda'}(\{\mathbf{l}_i\}; \mathbf{P}, \mathbf{P}') = F^{\lambda\lambda'}(\mathbf{l}_1, \mathbf{l}_2, \mathbf{l}_3) \delta^{(2)}\left(\sum_i \mathbf{l}_i + \mathbf{P} - \mathbf{P}'\right). \quad (45)$$

We impose the normalization condition:

$$F^{\lambda\lambda'}(\mathbf{l}_1, \mathbf{l}_2, \mathbf{l}_3)|_{\mathbf{l}_1=\mathbf{l}_2=\mathbf{l}_3=0} = \delta^{\lambda\lambda'}. \quad (46)$$

Correspondingly, we also extract a delta function from the impact factor:

$$\mathcal{B}_N^{\lambda\lambda'}(\{\mathbf{l}_i\}; \mathbf{P}, \mathbf{P}') = B_N^{\lambda\lambda'}(\{\mathbf{l}_i\}) \delta^{(2)}\left(\sum_i \mathbf{l}_i + \mathbf{P} - \mathbf{P}'\right). \quad (47)$$

In the following we will restrict ourselves to the forward direction, $\mathbf{P} = \mathbf{P}' = 0$. Because of helicity conservation for the impact factor, we always have $\lambda = \lambda'$, and we will drop the upper helicity labels, i.e. $F^{\lambda\lambda'}(\mathbf{l}_1, \mathbf{l}_2, \mathbf{l}_3) \rightarrow F(\mathbf{l}_1, \mathbf{l}_2, \mathbf{l}_3)$ etc. We will go through the cases of $N = 2$, $N = 3$, and $N = 4$ gluons. We therefore define, for fixed N , the functions $B_{N;0}(\{\mathbf{l}_i\})$ projected on the C -even channel through

$$B_N^{\lambda\lambda}(\{\mathbf{l}_i\}; \mathbf{P}, \mathbf{P}')|_{\mathbf{P}=\mathbf{P}'=0}^{C\text{-even}} = B_{N;0}(\{\mathbf{l}_i\}) \delta^{(2)}\left(\sum_i \mathbf{l}_i\right), \quad (48)$$

and analogously for the C -odd projections $\tilde{B}_{N;0}$.

In the remaining part of this section the main emphasis will be on the color structure of the impact factors, contained in (44). As the main result, we will find a decomposition into a sum of terms that, as will be demonstrated in the subsequent section, stays invariant under evolution in rapidity. We stress that the results that follow are valid for an arbitrary overlap function $F(\mathbf{l}_1, \mathbf{l}_2, \mathbf{l}_3)$, i.e. they do not rely on a particular model of the baryon wave function, provided the baryon has the valence degrees of freedom of three quarks.

4.2 Two gluons

We begin with the two-gluon coupling, which is C -even. All diagrams are proportional the color tensor $\delta^{a_1 a_2}$, and it is suggestive to group them into three sets: in the first one, the two gluons couple to the quark pair (12), and quark 3 acts as a spectator (Fig. 12). In the second one the gluons couple to (13) and quark 2 acts as spectator etc. Inside each set, we have four terms. We thus find

$$B_{2;0}(\mathbf{k}_1, \mathbf{k}_2) = \delta^{a_1 a_2} \left[D_{2;0}^{\{1,2\}}(\mathbf{k}_1, \mathbf{k}_2) + D_{2;0}^{\{1,3\}}(\mathbf{k}_1, \mathbf{k}_2) + D_{2;0}^{\{2,3\}}(\mathbf{k}_1, \mathbf{k}_2) \right], \quad (49)$$

with

$$D_{2;0}^{\{1,2\}}(\mathbf{k}_1, \mathbf{k}_2) = \frac{-g^2}{12} [F(\mathbf{k}, 0, 0) + F(0, \mathbf{k}, 0) - F(\mathbf{k}_1, \mathbf{k}_2, 0) - F(\mathbf{k}_2, \mathbf{k}_1, 0)], \quad (50)$$

$$D_{2;0}^{\{1,3\}}(\mathbf{k}_1, \mathbf{k}_2) = \frac{-g^2}{12} [F(\mathbf{k}, 0, 0) + F(0, 0, \mathbf{k}) - F(\mathbf{k}_1, 0, \mathbf{k}_2) - F(\mathbf{k}_2, 0, \mathbf{k}_1)], \quad (51)$$

$$D_{2;0}^{\{2,3\}}(\mathbf{k}_2, \mathbf{k}_3) = \frac{-g^2}{12} [F(0, \mathbf{k}, 0) + F(0, 0, \mathbf{k}) - F(0, \mathbf{k}_1, \mathbf{k}_2) - F(0, \mathbf{k}_2, \mathbf{k}_1)], \quad (52)$$

where \mathbf{k}_1 , \mathbf{k}_2 denote the gluon momenta and $\mathbf{k} = \mathbf{k}_1 + \mathbf{k}_2$. On the r.h.s. of (50)–(52), the momentum arguments

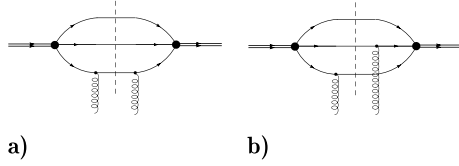


Fig. 12. Diagrams defining $B_{2;0}$

of the F functions indicate which diagrams they represent: in the first (second) term of (50), both gluons couple to quark line 1 (2). In the third term, the first gluon couples to line 1, the second to line 2, and so on. The relative signs arise from the color structure. As a striking result, on the r.h.s. of (50)–(52), in each line the four terms have the same structure as the impact factor of the photon. In particular, each set satisfies the Ward identities, i.e. it vanishes as any of its momenta goes to zero. Since the pair of scattering quarks $\{i, j\}$ is in a color anti-triplet state, one might, at first sight, interpret this set as the elastic scattering of an ‘anti-triplet dipole’. However, it is important to stress that these three dipole-like components, $D_{2;0}^{\{i,j\}}$, are not independent from each other: the diagrams where two gluons couple to the same quark line, say, line 3 in Fig. 12a, contribute both to the pair (13) and (23). In this sense, one better views these quark pairs as ‘anti-triplets inside the baryon’. Also, these configurations where one quark pair interacts whereas the third quark remains a spectator, should not simply be viewed as ‘diquark states’: in transverse coordinate space, the spectator quark can be far away from the quark pair (see the discussion in Sect. 7). One should also add that the normalization of the dipole-like components $D_{2;0}^{\{i,j\}}$ of the baryon impact factor is exactly 1/2 of the normalization of the genuine color dipole impact factor. At the two-gluon level, our results coincide with results of [47, 48].

If, instead of our model for the baryonic impact factor, we would have used a completely symmetric baryon form factor $F^{(s)}$ (which does not discriminate between u and d quarks) we would have arrived at the familiar result [49]:

$$B_{2;0}^{(s)}(\mathbf{k}_1, \mathbf{k}_2) = \frac{-g^2}{2} \delta^{a_1 a_2} [F^{(s)}(\mathbf{k}, 0, 0) - F^{(s)}(\mathbf{k}_1, \mathbf{k}_2, 0)] . \quad (53)$$

4.3 Three gluons

In the case of three gluons (Fig. 13) we have to distinguish between even and odd C parity: in the color trace (44) we find both color tensors, $f^{a_1 a_2 a_3}$ and $d^{a_1 a_2 a_3}$. The first one belongs to even (pomeron), the second to odd (odderon) C parity.

The C -odd baryon impact factor reads [33, 50–52]

$$\tilde{B}_{3;0}(\mathbf{k}_1, \mathbf{k}_2, \mathbf{k}_3) = d^{a_1 a_2 a_3} E_{3;0}(\mathbf{k}_1, \mathbf{k}_2, \mathbf{k}_3) , \quad (54)$$

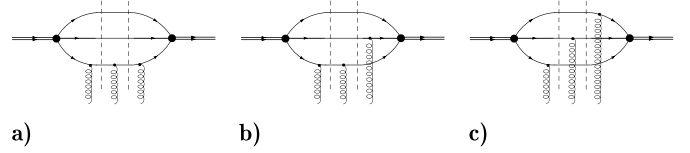


Fig. 13. Examples of diagrams defining $B_{3;0}$ and $\tilde{B}_{3;0}$

where

$$E_{3;0}(\mathbf{k}_1, \mathbf{k}_2, \mathbf{k}_3) = \frac{ig^3}{24} \sum_{\sigma} \left[2F^{\sigma}(\mathbf{k}_1, \mathbf{k}_2, \mathbf{k}_3) - \sum_{i=1}^3 F^{\sigma}(\mathbf{k}_i, \mathbf{k} - \mathbf{k}_i, 0) + F^{\sigma}(\mathbf{k}, 0, 0) \right] , \quad (55)$$

and F^{σ} denotes the F functions, with its arguments being permuted by the permutation σ :

$$F^{\sigma}(\mathbf{l}_1, \mathbf{l}_2, \mathbf{l}_3) = F(\mathbf{l}_{\sigma(1)}, \mathbf{l}_{\sigma(2)}, \mathbf{l}_{\sigma(3)}) . \quad (56)$$

In $E_{3;0}$ the t -channel three-gluon state is Bose symmetric, that is

$$E_{3;0}(\mathbf{k}_{\sigma(1)}, \mathbf{k}_{\sigma(2)}, \mathbf{k}_{\sigma(3)}) = E_{3;0}(\mathbf{k}_1, \mathbf{k}_2, \mathbf{k}_3) \quad (57)$$

for any permutation σ , and it obeys the Ward identities:

$$E_{3;0}(\mathbf{k}_1, \mathbf{k}_2, \mathbf{k}_3) = 0 \quad \text{for any } \mathbf{k}_j \rightarrow 0 . \quad (58)$$

On the r.h.s. of (55), the momentum structure of first term indicates that the three gluons couple to three quarks. The second and third term play the role of subtractions. This leads to the interpretation that, in this piece of the baryonic impact factor, in contrast to the structure found previously for 2 gluons, all three quarks participate in the interaction. Since each of the three gluons has negative C parity, this t -channel belongs to the $C = -$ (odderon) state.

For a completely symmetric model for the baryon form factor expression (55), again, reduces to a known result [50, 51]:

$$\tilde{B}_{3;0}^{(s)}(\mathbf{k}_1, \mathbf{k}_2, \mathbf{k}_3) = \frac{ig^3}{4} d^{a_1 a_2 a_3} \left[2F^{(s)}(\mathbf{k}_1, \mathbf{k}_2, \mathbf{k}_3) - \sum_{i=1}^3 F^{(s)}(\mathbf{k}_i, \mathbf{k} - \mathbf{k}_i, 0) + F^{(s)}(\mathbf{k}, 0, 0) \right] . \quad (59)$$

Next we turn to the terms proportional to $f^{a_1 a_2 a_3}$, which turn out to belong to even C . They can be grouped in the same ‘dipole-like’ form as in (49):

$$B_{3;0}(\mathbf{k}_1, \mathbf{k}_2, \mathbf{k}_3) = D_{3;0}^{\{1,2\}}(\mathbf{k}_1, \mathbf{k}_2, \mathbf{k}_3) + D_{3;0}^{\{1,3\}}(\mathbf{k}_1, \mathbf{k}_2, \mathbf{k}_3) + D_{3;0}^{\{2,3\}}(\mathbf{k}_1, \mathbf{k}_2, \mathbf{k}_3) , \quad (60)$$

where the dipole-like components have the structure known from the photon case,

$$D_{3;0}^{\{i,j\}}(\mathbf{k}_1, \mathbf{k}_2, \mathbf{k}_3) = \frac{1}{2} g f^{a_1 a_2 a_3} \left[D_{2;0}^{\{i,j\}}(\mathbf{k}_1 + \mathbf{k}_2, \mathbf{k}_3) - D_{2;0}^{\{i,j\}}(\mathbf{k}_1 + \mathbf{k}_3, \mathbf{k}_2) + D_{2;0}^{\{i,j\}}(\mathbf{k}_2 + \mathbf{k}_3, \mathbf{k}_1) \right]. \quad (61)$$

As in the photon case, the structure of the argument indicates the beginning of the reggeization of the gluons: for example, in the first term, the first two gluons with momenta \mathbf{k}_1 and \mathbf{k}_2 ‘collapse’ into a single reggeized gluon with momentum $\mathbf{k}_1 + \mathbf{k}_2$. The t -channel system thus consists of two reggeized gluons only and hence belongs to C -even. In the next section we will show that this structure is preserved in the rapidity evolution.

In the following it will be convenient to use a short-hand notation by writing, instead of $D_{2;0}^{\{i,j\}}(\mathbf{k}_1 + \mathbf{k}_2, \mathbf{k}_3)$, simply $D_{2;0}^{\{i,j\}}(12, 3)$ etc.

4.4 Four gluons

In the case of four gluons (Fig. 14) the color trace (44) contains ff , dd , fd , and $\delta\delta$ color tensor structures. Beginning with the fd pieces, we find that they can be expressed in terms of the E -function (55), which we have obtained for the odderon channel:

$$\begin{aligned} \tilde{B}_{4;0}(1, 2, 3, 4) = & \frac{g}{2} (f^{a_1 a_2 b} d^{ba_3 a_4} E_{3;0}(12, 3, 4) + f^{a_1 a_3 b} d^{ba_2 a_4} E_{3;0}(13, 2, 4) \\ & + f^{a_1 a_4 b} d^{ba_2 a_3} E_{3;0}(14, 2, 3) + f^{a_2 a_3 b} d^{ba_1 a_4} E_{3;0}(23, 1, 4) \\ & + f^{a_2 a_4 b} d^{ba_1 a_3} E_{3;0}(24, 1, 3) + f^{a_3 a_4 b} d^{ba_1 a_2} E_{3;0}(34, 1, 2)). \end{aligned} \quad (62)$$

We then interpret this contribution as the odderon configuration with one reggeized gluon. It agrees with the result first found by Ewerz [33].

Next the ff , dd , and $\delta\delta$ terms. We find, in addition to a set of pieces, which have the same structure as in the photon case, a new structure, $Q_{4;0}$. In detail:

$$\begin{aligned} B_{4;0}(1, 2, 3, 4) = & D_{4;0}^{\{1,2\}}(1, 2, 3, 4) + D_{4;0}^{\{1,3\}}(1, 2, 3, 4) \\ & + D_{4;0}^{\{2,3\}}(1, 2, 3, 4) + Q_{4;0}(1, 2, 3, 4). \end{aligned} \quad (63)$$

Here the first three terms are dipole-like, and they follow the reggeization pattern found for the photon scattering:

$$D_{4;0}^{\{i,j\}}(1, 2, 3, 4) = -g^2 \left\{ d^{a_1 a_2 a_3 a_4} \left[D_{2;0}^{\{i,j\}}(123, 4) + D_{2;0}^{\{i,j\}}(234, 1) - D_{2;0}^{\{i,j\}}(14, 23) \right] \right.$$

$$\left. + d^{a_1 a_2 a_3 a_4} \left[D_{2;0}^{\{i,j\}}(124, 3) + D_{2;0}^{\{i,j\}}(134, 2) - D_{2;0}^{\{i,j\}}(12, 34) - D_{2;0}^{\{i,j\}}(13, 24) \right] \right\}, \quad (64)$$

with the color tensor

$$d^{a_1 a_2 a_3 a_4} = \frac{\delta^{a_1 a_2} \delta^{a_3 a_4}}{2N_c} + \frac{d^{a_1 a_2 b} d^{ba_3 a_4}}{4} - \frac{f^{a_1 a_2 b} f^{ba_3 a_4}}{4}. \quad (65)$$

In the next section we will study the rapidity evolution of these terms, and we will confirm that they follow the photon impact factor to all orders.

The new structure, which has no analogue in the case of the photon looks as follows:

$$\begin{aligned} Q_{4;0}(1, 2, 3, 4) = & \frac{-ig}{2} \left[d^{a_1 a_2 b} d^{ba_3 a_4} - \frac{1}{3} \delta^{a_1 a_2} \delta^{a_3 a_4} \right] \\ & \times [E_{3;0}(12, 3, 4) + E_{3;0}(34, 1, 2)] \\ & + \frac{-ig}{2} \left[d^{a_1 a_3 b} d^{ba_2 a_4} - \frac{1}{3} \delta^{a_1 a_3} \delta^{a_2 a_4} \right] \\ & \times [E_{3;0}(13, 2, 4) + E_{3;0}(24, 1, 3)] \\ & + \frac{-ig}{2} \left[d^{a_1 a_4 b} d^{ba_2 a_3} - \frac{1}{3} \delta^{a_1 a_4} \delta^{a_2 a_3} \right] \\ & \times [E_{3;0}(14, 2, 3) + E_{3;0}(23, 1, 4)]. \end{aligned} \quad (66)$$

The function E is the same as in the odderon case, and, in particular, all three quarks participate in the interaction. The t -channel state that couples to $Q_{4;0}$ is Bose symmetric,

$$Q_{4;0}(\sigma(1), \sigma(2), \sigma(3), \sigma(4)) = Q_{4;0}(1, 2, 3, 4) \quad (67)$$

for any permutation σ , and it is gauge invariant,

$$Q_{4;0}(\mathbf{k}_1, \mathbf{k}_2, \mathbf{k}_3, \mathbf{k}_4) = 0 \quad \text{for any } \mathbf{k}_j \rightarrow 0. \quad (68)$$

This property may be proven using the identity for color tensors valid for $N_c = 3$:

$$\begin{aligned} d^{a_1 a_2 b} d^{ba_3 a_4} + d^{a_1 a_3 b} d^{ba_2 a_4} + d^{a_1 a_4 b} d^{ba_2 a_3} \\ = \frac{1}{3} (\delta^{a_1 a_2} \delta^{a_3 a_4} + \delta^{a_1 a_3} \delta^{a_2 a_4} + \delta^{a_1 a_4} \delta^{a_2 a_3}). \end{aligned} \quad (69)$$

The analysis in the following section will show that this novel piece of the baryon impact factor couples a three-gluon t -channel configuration in which one of the reggeized gluons is an even signature d reggeon. The overall C parity therefore is positive.

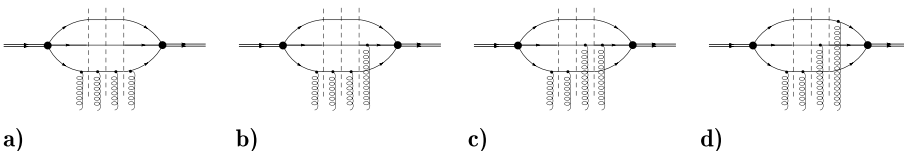


Fig. 14. Examples of diagrams defining $B_{4;0}$ and $\tilde{B}_{4;0}$

5 Integral evolution equations

In this section we study higher order corrections in the (generalized) leading logarithmic ($\log s$) approximation. The all order sum of these terms will be represented by integral equations [31, 32], written for the Mellin moments of the multiple discontinuities with respect to the energy s . In our notation the dependence of the amplitudes B_N and \tilde{B}_N (and also D_N , E_N and Q_N) on the Mellin variable ω is implicit.

Let us begin with the C -odd configurations. In the case of three gluons, the impact factor $E_{3,0}$ is simply replaced by the Green's function E_3 , which satisfies the BKP equation for three odd signature reggeons, with the initial condition given by $E_{3,0}$:

$$\left(\omega - \sum_i \beta(\mathbf{k}_i)\right) E_3 = E_{3,0} + \sum_{(r,s)} K_{2 \rightarrow 2}(r, s) \otimes E_3, \quad (70)$$

where $K_{2 \rightarrow 2}$ is the real emission part of the BFKL kernel, and the odderon state with the full color structure reads

$$\tilde{B}_3(1, 2, 3) = d^{a_1 a_2 a_3} E_3(1, 2, 3). \quad (71)$$

The four-gluon case has been studied in [33], and we simply quote the solution:

$$\begin{aligned} \tilde{B}_4(1, 2, 3, 4) = & \frac{g}{2} [f^{a_1 a_2 b} d^{b a_3 a_4} E_3(12, 3, 4) + f^{a_1 a_3 b} d^{b a_2 a_4} E_3(13, 2, 4) \\ & + f^{a_1 a_4 b} d^{b a_2 a_3} E_3(14, 2, 3) + f^{a_2 a_3 b} d^{b a_1 a_4} E_3(23, 1, 4) \\ & + f^{a_2 a_4 b} d^{b a_1 a_3} E_3(24, 1, 3) + f^{a_3 a_4 b} d^{b a_1 a_2} E_3(34, 1, 2)], \end{aligned} \quad (72)$$

where the function E_3 has been defined before in (70). Clearly, the solution is saturated by a reggeizing contribution: in each term, one of the three f reggeons splits into two elementary gluons.

We now turn to the C -even contributions. The integral equations for the multiple discontinuities read (up to four gluons)

$$\left(\omega - \sum_i \beta(\mathbf{k}_i)\right) B_2 = B_{2,0} + \text{diagram}, \quad (73)$$

$$\begin{aligned} \left(\omega - \sum_i \beta(\mathbf{k}_i)\right) B_3 = & B_{3,0} + \sum \text{diagram} \\ & + \text{diagram}, \end{aligned} \quad (74)$$

$$\begin{aligned} \left(\omega - \sum_i \beta(\mathbf{k}_i)\right) B_4 = & B_{4,0} + \sum \text{diagram} \\ & + \sum \text{diagram} + \text{diagram}. \end{aligned} \quad (75)$$

The integral kernels driving $2 \rightarrow 2, 3, 4, \dots$ reggeon transitions that appear in the above equations include the color structure, and they are defined in [31, 32]. The gluon Regge trajectory $\beta(\mathbf{k})$ will be specified below. The case of two gluons is the simplest one: B_2 satisfies the BFKL equation. According to the structure of the inhomogeneous term in (49), B_2 can be written as the sum of three terms $D_2^{\{i,j\}}$,

$$B_2(1, 2) = \delta^{a_1 a_2} [D_2^{\{1,2\}}(1, 2) + D_2^{\{1,3\}}(1, 2) + D_2^{\{2,3\}}(1, 2)], \quad (76)$$

with

$$\left(\omega - \sum_{i=1}^2 \beta(\mathbf{k}_i)\right) D_2^{\{i,j\}} = D_{2,0}^{\{i,j\}} + K_{2 \rightarrow 2} \otimes D_2^{\{i,j\}}. \quad (77)$$

In the case of three gluons, B_3 is given by the sum of three dipole-like components (cf. (60)):

$$\begin{aligned} B_3(1, 2, 3) = & D_3^{\{1,2\}}(1, 2, 3) + D_3^{\{1,3\}}(1, 2, 3) \\ & + D_3^{\{2,3\}}(1, 2, 3), \end{aligned} \quad (78)$$

where each term consists of three reggeizing pieces:

$$\begin{aligned} D_3^{\{i,j\}}(1, 2, 3) = & \frac{1}{2} g f^{a_1 a_2 a_3} [D_2^{\{i,j\}}(12, 3) - D_2^{\{i,j\}}(13, 2) \\ & + D_2^{\{i,j\}}(23, 1)]. \end{aligned} \quad (79)$$

This structure coincides with the photon case.

The case of B_4 is more complex. Following our result for the baryon impact factor in (63) we decompose B_4 in the following way:

$$\begin{aligned} B_4(1, 2, 3, 4) = & D_4^{\{1,2\}}(1, 2, 3, 4) + D_4^{\{1,3\}}(1, 2, 3, 4) \\ & + D_4^{\{2,3\}}(1, 2, 3, 4) + Q_4(1, 2, 3, 4). \end{aligned} \quad (80)$$

For the dipole-like pieces $D_4^{\{i,j\}}$ we make use of the 'reduction procedure' developed for the photon case. Namely we decompose each $D_4^{\{i,j\}}$ into a reggeizing and an irreducible contributions

$$D_4^{\{i,j\}}(1, 2, 3, 4) = D_4^{\{i,j\};R}(1, 2, 3, 4) + D_4^{\{i,j\};I}(1, 2, 3, 4), \quad (81)$$

with the reggeizing contribution given by

$$\begin{aligned} D_4^{\{i,j\};R}(1, 2, 3, 4) = & -g^2 \{ d^{a_1 a_2 a_3 a_4} [D_2^{\{i,j\}}(123, 4) + D_2^{\{i,j\}}(234, 1) \\ & - D_2^{\{i,j\}}(14, 23)] \\ & + d^{a_1 a_2 a_4 a_3} [D_2^{\{i,j\}}(124, 3) + D_2^{\{i,j\}}(134, 2) \\ & - D_2^{\{i,j\}}(12, 34) - D_2^{\{i,j\}}(13, 24)] \}. \end{aligned} \quad (82)$$

The reggeizing contributions are simple BFKL ladders with one reggeizing gluon splitting into three gluons or both reggeized gluons each splitting into two gluons. The

irreducible contribution, containing the $2 \rightarrow 4$ reggeon transition vertex, is illustrated in Fig. 15.

These results provide further evidence that the ‘dipole-like’ pieces of the baryonic impact factor really behave in exactly the same way as the color dipole photon impact factor. In particular, if we would apply the large N_c limit to the gluon evolution below the impact factor (which, of course, would be inconsistent with our finite- N_c baryon), the four-gluon system below the $2 \rightarrow 4$ transition vertex would split into two non-interacting BFKL ladders, and we would arrive at the first iteration of the BK equation.

After subtracting from $B_4(1, 2, 3, 4)$ in (80) these dipole-like contributions of the baryon we are left with Q_4 . As Q_4 appears at the level of four gluons, its evolution equation simply has the BKP form:

$$\left(\omega - \sum_i \beta(\mathbf{k}_i)\right) \begin{array}{c} \text{---} \text{---} \text{---} \text{---} \\ \text{---} \text{---} \text{---} \text{---} \\ \text{---} \text{---} \text{---} \text{---} \\ \text{---} \text{---} \text{---} \text{---} \end{array} Q_4 = \begin{array}{c} \text{---} \text{---} \text{---} \text{---} \\ \text{---} \text{---} \text{---} \text{---} \\ \text{---} \text{---} \text{---} \text{---} \\ \text{---} \text{---} \text{---} \text{---} \end{array} Q_{4;0} + \sum \begin{array}{c} \text{---} \text{---} \text{---} \text{---} \\ \text{---} \text{---} \text{---} \text{---} \\ \text{---} \text{---} \text{---} \text{---} \\ \text{---} \text{---} \text{---} \text{---} \end{array} Q_4. \quad (83)$$

Making use of the experience with D_4 , we decompose the amplitude Q_4 into a reggeizing piece Q_4^R and an irreducible contribution Q_4^I :

$$Q_4(1, 2, 3, 4) = Q_4^R(1, 2, 3, 4) + Q_4^I(1, 2, 3, 4). \quad (84)$$

Going through steps similar to the ones outlined in [31, 32] we find that the reggeizing pieces Q_4^R preserve the structure of $Q_{4;0}$:

$$\begin{aligned} Q_4^R(1, 2, 3, 4) = & \frac{-ig}{2} \left[d^{a_1 a_2 b} d^{b a_3 a_4} - \frac{1}{3} \delta^{a_1 a_2} \delta^{a_3 a_4} \right] \\ & \times [E_3(12, 3, 4) + E_3(34, 1, 2)] \\ & + \frac{-ig}{2} \left[d^{a_1 a_3 b} d^{b a_2 a_4} - \frac{1}{3} \delta^{a_1 a_3} \delta^{a_2 a_4} \right] \\ & \times [E_3(13, 2, 4) + E_3(24, 1, 3)] \\ & + \frac{-ig}{2} \left[d^{a_1 a_4 b} d^{b a_2 a_3} - \frac{1}{3} \delta^{a_1 a_4} \delta^{a_2 a_3} \right] \\ & \times [E_3(14, 2, 3) + E_3(23, 1, 4)]. \end{aligned} \quad (85)$$

As seen from the color and momentum structure, the three-gluon state coupling to $Q_{4;0}$ consists of three reggeized

gluons, one of which is in a d state and decays into two elementary gluons (the pieces proportional to color tensors $\delta\delta$ play the role of subtractions; in particular, they are needed in order to satisfy the Ward identities). This state, consisting of two odd signature f reggeon and one even signature d reggeon, belongs to even C , i.e. to the pomeron channel.

The remaining piece, Q_4^I , contains a new transition vertex. We illustrate this contribution in Fig. 16. This vertex describes the transition from the three-reggeon state consisting of two f reggeons and one d reggeon to four f reggeons. In more detail, the vertex may be completely decomposed into non-connected pieces of two types: (i) the incoming d reggeon together with one of the f reggeons makes a transition into three f reggeons, whereas the remaining f reggeon acts as a (t -channel) spectator, and (ii) two f reggeons interact via the BFKL kernel and the d reggeon splits into two f reggeons. The explicit functional form of the vertex W , acting on the three-reggeon state ϕ_3 is the following:

$$\begin{aligned} (W\phi_3)(1, 2, 3, 4) = & \frac{-g^2}{2} \left[\delta^{a_1 a_2} \delta^{a_3 a_4} \mathcal{W}\phi_3^{1234} \right. \\ & \left. + \delta^{a_1 a_3} \delta^{a_2 a_4} \mathcal{W}\phi_3^{1324} + \delta^{a_1 a_4} \delta^{a_2 a_3} \mathcal{W}\phi_3^{1423} \right], \end{aligned} \quad (86)$$

where

$$\begin{aligned} \mathcal{W}\phi_3 = & \left[\mathcal{G}\phi_3^{123\cdots 4} + \mathcal{G}\phi_3^{213\cdots 4} + \mathcal{G}\phi_3^{132\cdots 4} - \mathcal{G}\phi_3^{(12)\circ 3\cdots 4} + \frac{1}{2} \mathcal{G}\phi_3^{1\circ 2\cdots (34)} \right] \\ & + [3 \leftrightarrow 4] + [1 \leftrightarrow 3, 2 \leftrightarrow 4] + [1 \leftrightarrow 4, 2 \leftrightarrow 3]. \end{aligned} \quad (87)$$

Let us stress that this vertex acts on a completely symmetric function ϕ_3 with three arguments, which inherits its structure from E_3 . This vertex is closely related to the $3 \rightarrow 4$ vertex found in [53, 54] in an analysis of jet production amplitudes at small x . The symbol \mathcal{G} denotes the integral operator $G(1, 2, 3)$, introduced first in [31] and further investigated in [55]. It acts on a two-gluon amplitude, ϕ_2 and describes a transition to three gluons. It consists of two pieces:

$$G(1, 2, 3) = G_1(1, 2, 3) + G_2(1, 2, 3), \quad (88)$$

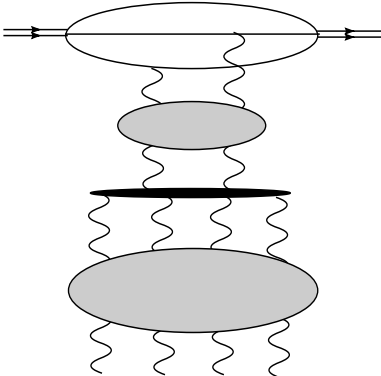


Fig. 15. The component $D_4^{\{i,j\};I}(1, 2, 3, 4)$

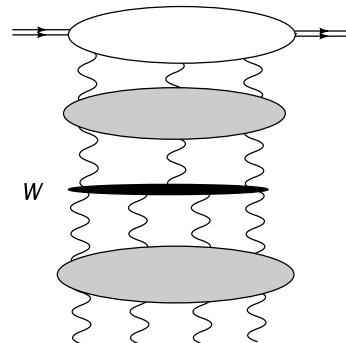


Fig. 16. The new $3 \rightarrow 4$ transition vertex W

where the first one contains s -channel gluons ('connected part'), the second one reggeizing pieces ('disconnected part'):

$$(G_1\phi_2)(\mathbf{k}_1, \mathbf{k}_2, \mathbf{k}_3) = \int \frac{d^2l}{(2\pi)^3} \left(\frac{(\mathbf{k}_2 + \mathbf{k}_3)^2 l^2}{(1 - \mathbf{k}_1)^2} + \frac{(\mathbf{k}_1 + \mathbf{k}_2)^2 (\mathbf{k} - 1)^2}{(\mathbf{k} - 1 - \mathbf{k}_3)^2} - \frac{\mathbf{k}_2^2 (\mathbf{k} - 1)^2 l^2}{(1 - \mathbf{k}_1)^2 (\mathbf{k} - 1 - \mathbf{k}_3)^2} - \mathbf{k}^2 \right) \phi_2(1, \mathbf{k} - 1), \quad (89)$$

and

$$N_c g^2 (G_2\phi_2)(\mathbf{k}_1, \mathbf{k}_2, \mathbf{k}_3) = \int \frac{d^2l}{(2\pi)^3} l^2 (\mathbf{k} - 1)^2 \{ [\beta(\mathbf{k}_2 + \mathbf{k}_3) - \beta(\mathbf{k}_2)] (2\pi)^3 \delta^{(2)}(1 - \mathbf{k}_1) + [\beta(\mathbf{k}_1 + \mathbf{k}_2) - \beta(\mathbf{k}_2)] (2\pi)^3 \delta^{(2)}(1 - \mathbf{k}_3) \} \phi_2(1, \mathbf{k} - 1), \quad (90)$$

with the gluon trajectory function

$$\beta(\mathbf{k}_i) = -N_c g^2 \int \frac{d^2l}{(2\pi)^3} \frac{\mathbf{k}_i^2}{l^2 + (\mathbf{k}_i - 1)^2} \frac{1}{(\mathbf{k}_i - 1)^2}, \quad (91)$$

and $\mathbf{k} = \mathbf{k}_1 + \mathbf{k}_2 + \mathbf{k}_3$. In (87) we have used a short-hand notation for the argument structure introduced in [53, 54]:

in the first term $\overset{123 \cdots 4}{\mathcal{G}} \phi_3$, ϕ_3 is the three-gluon amplitude above the vertex W where the rightmost reggeon (momentum \mathbf{k}_4) is a spectator, and the G operator acts on the two left reggeons, turning them into the three gluons with momenta $\mathbf{k}_1, \mathbf{k}_2$, and \mathbf{k}_3 . In the fourth term $\overset{(12) \circ 3 \cdots 4}{\mathcal{G}} \phi_3$, reggeon 4 is, again, a spectator, and the G operator (with zero momentum in the second outgoing gluon) equals the BFKL kernel acting on the two leftmost gluons inside ϕ_3 : after this BFKL interaction the leftmost gluon splits into two gluons with momenta \mathbf{k}_1 and \mathbf{k}_2 , and the other one carries momentum \mathbf{k}_3 . Finally, in the last term $\overset{1 \circ 2 \cdots (34)}{\mathcal{G}} \phi_3$, the rightmost spectator now splits into two gluons with momenta \mathbf{k}_3 and \mathbf{k}_4 , and the G operator, like in the previous term, equals the BFKL operator with outgoing momenta \mathbf{k}_1 and \mathbf{k}_2 .

The full vertex W in (86) is gauge invariant, infrared finite and Bose symmetric. As the vertex is expressed in terms of the function \mathcal{G} , it is also Möbius invariant [55]. Finally, there is no violation of signature conservation: the incoming three-reggeon state, consisting of one d reggeon and two f reggeons, has even signature; the same holds for the outgoing four-reggeon state (four f reggeons).

As a result, the baryonic impact factor introduces a new contribution to the pomeron channel, which has no analogue in the photon dipole factor.

6 Baryon wave functions in the coordinate space

The baryon wave function in transverse position space may be easily obtained by the Fourier transform:

$$\begin{aligned} \tilde{\Psi}_\lambda^{(\lambda_1, \lambda_2) \lambda_3}(\{\alpha_i\}, \{\mathbf{r}_i\}; \mathbf{P}) &= \int \frac{d^2p_1}{2\pi} \frac{d^2p_2}{2\pi} \frac{d^2p_3}{2\pi} \\ &\times \Psi_\lambda^{(\lambda_1, \lambda_2) \lambda_3}(\{\alpha_i\}, \{\mathbf{p}_i\}; \mathbf{P}) \exp\left(i \sum_{i=1}^3 \mathbf{p}_i \cdot \mathbf{r}_i\right). \end{aligned} \quad (92)$$

The result takes a rather simple form:

$$\begin{aligned} \tilde{\Psi}_\lambda^{(\lambda_1, \lambda_2) \lambda_3}(\{\alpha_i\}, \{\mathbf{r}_i\}; \mathbf{P}) &= \tilde{\mathcal{N}} \alpha_1 \alpha_2 \alpha_3 \exp\left[-\frac{M^2}{4} \sum_i \alpha_i (\mathbf{r}_i - \mathbf{R})^2\right] \exp(i\mathbf{P} \cdot \mathbf{R}) \\ &\times \left\{ \lambda M \delta_{\lambda, \lambda_1} \delta_{\lambda, -\lambda_2} \delta_{\lambda, \lambda_3} [(\mathbf{r}_2 - \mathbf{R}) \cdot \boldsymbol{\eta}_\lambda] [(\mathbf{r}_1 - \mathbf{r}_3) \cdot \boldsymbol{\eta}_{-\lambda}] \right. \\ &+ \lambda M \delta_{\lambda, -\lambda_1} \delta_{\lambda, \lambda_2} \delta_{\lambda, \lambda_3} [(\mathbf{r}_1 - \mathbf{R}) \cdot \boldsymbol{\eta}_\lambda] [(\mathbf{r}_2 - \mathbf{r}_3) \cdot \boldsymbol{\eta}_{-\lambda}] \\ &- 2i \delta_{\lambda, \lambda_1} \delta_{\lambda, -\lambda_2} \delta_{\lambda, -\lambda_3} [(\mathbf{r}_2 - \mathbf{r}_3) \cdot \boldsymbol{\eta}_\lambda] \\ &\left. - 2i \delta_{\lambda, -\lambda_1} \delta_{\lambda, \lambda_2} \delta_{\lambda, -\lambda_3} [(\mathbf{r}_1 - \mathbf{r}_3) \cdot \boldsymbol{\eta}_\lambda] \right\}, \end{aligned} \quad (93)$$

where \mathbf{R} denotes the light-cone center of mass position vector,

$$\mathbf{R} = \sum_{i=1}^3 \alpha_i \mathbf{r}_i. \quad (94)$$

The form of the wave function given by (93), which follows from the Ioffe current, shows in detail the angular momentum structure of the baryon and the correlations between the angular momenta and quark helicities. In particular, each scalar product of the type $(\mathbf{r}_1 - \mathbf{R}) \cdot \boldsymbol{\eta}_\lambda$ clearly indicates a rotation of quark 1 around the baryon center of mass with the orbital angular momentum z -component, L_z , equal to λ . Terms of the type $(\mathbf{r}_1 - \mathbf{r}_3) \cdot \boldsymbol{\eta}_\lambda$ correspond to a similar rotation within the quark pair (1,3). Thus, in the massless quark case, all components of the baryon carry a non-zero angular momentum L_z for the Ioffe operator. An inspection of the momentum space expressions (32) shows that for the massive quark case, one may have Ioffe baryon wave function components with $L_z = 0$.

Using (43) and (39), one may express the baryon impact factors $\mathcal{B}_N^{\lambda\lambda'}(\{\mathbf{l}_i\}; \mathbf{P}, \mathbf{P}')$ via the overlap function $\mathcal{F}^{\lambda\lambda'}(\{\mathbf{l}_i\}; \mathbf{P}, \mathbf{P}')$ defined in the coordinate space:

$$\begin{aligned} \mathcal{F}^{\lambda\lambda'}(\{\mathbf{l}_i\}; \mathbf{P}, \mathbf{P}') &= \sum_{\lambda_1, \lambda_2, \lambda_3} \int [d^2\mathbf{r}_i] [d\alpha_i] \\ &\times [\tilde{\Psi}_{\lambda'}^{(\lambda_1, \lambda_2) \lambda_3}(\{\alpha_i\}, \{\mathbf{r}_i\}; \mathbf{P}')]^* \exp\left(-i \sum_{i=1}^3 \mathbf{l}_i \cdot \mathbf{r}_i\right) \\ &\times \tilde{\Psi}_\lambda^{(\lambda_1, \lambda_2) \lambda_3}(\{\alpha_i\}, \{\mathbf{r}_i\}; \mathbf{P}). \end{aligned} \quad (95)$$

It follows from (45), (46) and (95) that the normalization condition for the wave function reads

$$\sum_{\lambda_1, \lambda_2, \lambda_3} \int [d^2 \mathbf{r}_i] [d\alpha_i] [\tilde{\Psi}_{\lambda}^{(\lambda_1, \lambda_2) \lambda_3}(\{\alpha_i\}, \{\mathbf{r}_i\}; \mathbf{P}')]^* \times \tilde{\Psi}_{\lambda}^{(\lambda_1, \lambda_2) \lambda_3}(\{\alpha_i\}, \{\mathbf{r}_i\}; \mathbf{P}) = \delta^{(2)}(\mathbf{P} - \mathbf{P}'). \quad (96)$$

It is instructive to evaluate a contribution to the baryon two-gluon impact factor $[\delta \mathcal{B}_{2;0}^{\lambda \lambda'}]^{1,2\}$ corresponding to a dipole-like piece, e.g. to $D_{2;0}^{\{1,2\}}$, in the coordinate representation. The gluon color labels are a_1 and a_2 and momenta are denoted by \mathbf{k}_1 and \mathbf{k}_2 respectively. One obtains

$$\begin{aligned} [\delta \mathcal{B}_{2;0}^{\lambda \lambda'}(\{\mathbf{l}_i\}; \mathbf{P}, \mathbf{P}')]^{1,2\} &= \frac{1}{2} (-ig)^2 \frac{\delta^{a_1 a_2}}{2N_c} \\ &\times \sum_{\lambda_1, \lambda_2, \lambda_3} \int [d^2 \mathbf{r}_i] [d\alpha_i] [\tilde{\Psi}_{\lambda'}^{(\lambda_1, \lambda_2) \lambda_3}(\{\alpha_i\}, \{\mathbf{r}_i\}; \mathbf{P}')]^* \\ &\times \tilde{\Psi}_{\lambda}^{(\lambda_1, \lambda_2) \lambda_3}(\{\alpha_i\}, \{\mathbf{r}_i\}; \mathbf{P}) [e^{-i(\mathbf{k}_1 + \mathbf{k}_2) \cdot \mathbf{r}_1} \\ &+ e^{-i(\mathbf{k}_1 + \mathbf{k}_2) \cdot \mathbf{r}_2} - e^{-i\mathbf{k}_1 \cdot \mathbf{r}_1 - i\mathbf{k}_2 \cdot \mathbf{r}_2} - e^{-i\mathbf{k}_1 \cdot \mathbf{r}_2 - i\mathbf{k}_2 \cdot \mathbf{r}_1}]. \end{aligned} \quad (97)$$

Assuming, for simplicity, the forward kinematics, $\mathbf{k}_1 = \mathbf{k} = -\mathbf{k}_2$, one may rewrite the eikonal factors in the last line of (97) in a factorized form, found in the case of the color dipole scattering,

$$[1 - e^{i\mathbf{k} \cdot (\mathbf{r}_2 - \mathbf{r}_1)}][1 - e^{i\mathbf{k} \cdot (\mathbf{r}_2 - \mathbf{r}_1)}]^*. \quad (98)$$

This equivalence of the structures holds also beyond the forward limit (note that, for non-zero \mathbf{P}, \mathbf{P}' the wave functions $\tilde{\Psi}_{\lambda'}^{(\lambda_1, \lambda_2) \lambda_3}$ contain the phase factors $e^{i\mathbf{P}\mathbf{R}}$). In (97), the prefactor $1/2$ in the first line reflects the relative weight between the color dipole scattering amplitude and the scattering amplitude of the dipole-like components of the baryon.

7 The quark–diquark limit

In many phenomenological applications the nucleon is represented as a bound state of quark and a tightly bound diquark. The transverse size of the diquark is then assumed to be much smaller than the size of the baryon, and the diquark state emerges in an anti-triplet color representation. In this approximation the baryon should resemble an (asymmetric) color dipole. It is interesting to analyze the properties of our baryon impact factor in this limit. Formally, the quark–diquark limit corresponds to the limit where the transverse separation of two quark lines shrinks to zero, and a t -channel gluon no longer distinguishes between the two quark lines. In momentum space, as seen in (95), the overlap function then only depends upon the sum of the momenta of all gluons coupled to the two coinciding quark lines. To be definite, let us assume that quarks 2 and 3 move close to each other. Then all overlap functions F degenerate to a function $F^{1(23)}$ with only two arguments:

$$F(\mathbf{k}_1, \mathbf{k}_2, \mathbf{k}_3) \xrightarrow{3 \rightarrow 2} F^{1(23)}(\mathbf{k}_1, \mathbf{k}_2 + \mathbf{k}_3) \quad (99)$$

(note that the limit $F^{1(23)}(\mathbf{k}_1, \mathbf{k}_2)$ is not necessarily symmetric in its arguments). Applying this argument to the three dipole-like terms in (49) we immediately see that the dipole-like component $D_{2;0}^{\{2,3\}}$ vanishes if lines 2 and 3 are contracted: this is the well-known limit of a dipole with vanishing size (color transparency). In more detail, (52) shows that all terms in this impact factor tend to $F^{1(23)}(0, \mathbf{k}_1 + \mathbf{k}_2)$, and they cancel due to opposite signs. The remaining dipole-like components $D_{2;0}^{\{1,2\}}$ and $D_{2;0}^{\{1,3\}}$ become equal:

$$D_{2;0}^{\{1,2\}}(\mathbf{k}_1, \mathbf{k}_2), D_{2;0}^{\{1,3\}}(\mathbf{k}_1, \mathbf{k}_2) \xrightarrow{3 \rightarrow 2} D_{2;0}^{\{1,(23)\}}(\mathbf{k}_1, \mathbf{k}_2), \quad (100)$$

with

$$\begin{aligned} D_{2;0}^{\{1,(23)\}}(\mathbf{k}_1, \mathbf{k}_2) &= \frac{-g^2}{12} [F^{1(23)}(0, \mathbf{k}_1 + \mathbf{k}_2) \\ &+ F^{1(23)}(\mathbf{k}_1 + \mathbf{k}_2, 0) - F^{1(23)}(\mathbf{k}_1, \mathbf{k}_2) - F^{1(23)}(\mathbf{k}_2, \mathbf{k}_1)]. \end{aligned} \quad (101)$$

As we already discussed at the end of Sect. 4.2, in (49) each dipole-like term carries a color factor $1/2$, compared to a genuine color dipole factor seen in a color singlet quark–antiquark system. Since in the quark–diquark limit $D_{2;0}^{\{2,3\}}$ vanishes and the contributions from $D_{2;0}^{\{1,2\}}$ and $D_{2;0}^{\{1,3\}}$ coincide, this part of the baryonic impact factor adds up to a standard dipole contribution $D_{2;0}(\mathbf{k}_1, \mathbf{k}_2) = 2D_{2;0}^{\{1,(23)\}}(\mathbf{k}_1, \mathbf{k}_2)$.

Next, we turn to the three-gluon impact factors. In the pomeron channel, one finds only reggeizing pieces of the quark–diquark dipole impact factor. In the odderon channel, the function $E(\mathbf{k}_1, \mathbf{k}_2, \mathbf{k}_3)$ degenerates to the structure found in the $\gamma^* \rightarrow \eta_c$ transition impact factor, which couples only to the Bartels–Lipatov–Vacca (BLV) odderon [56] but not to the Janik–Wosiek solution [57, 58]:

$$E_{3;0}(\mathbf{k}_1, \mathbf{k}_2, \mathbf{k}_3) \xrightarrow{3 \rightarrow 2} E_{3;0}^{\{1,(23)\}}(\mathbf{k}_1, \mathbf{k}_2, \mathbf{k}_3), \quad (102)$$

with

$$\begin{aligned} E_{3;0}^{\{1,(23)\}}(\mathbf{k}_1, \mathbf{k}_2, \mathbf{k}_3) &= \frac{ig^3}{12} [F^{1(23)}(\mathbf{k}_1, \mathbf{k}_2 + \mathbf{k}_3) - F^{1(23)}(\mathbf{k}_2 + \mathbf{k}_3, \mathbf{k}_1) \\ &+ F^{1(23)}(\mathbf{k}_2, \mathbf{k}_1 + \mathbf{k}_3) - F^{1(23)}(\mathbf{k}_1 + \mathbf{k}_3, \mathbf{k}_2) \\ &+ F^{1(23)}(\mathbf{k}_3, \mathbf{k}_1 + \mathbf{k}_2) - F^{1(23)}(\mathbf{k}_1 + \mathbf{k}_2, \mathbf{k}_3) \\ &+ F^{1(23)}(\mathbf{k}_1 + \mathbf{k}_2 + \mathbf{k}_3, 0) - F^{1(23)}(0, \mathbf{k}_1 + \mathbf{k}_2 + \mathbf{k}_3)]. \end{aligned} \quad (103)$$

For the four-gluon case, one finds the standard reggeizing pattern of $D_{2;0}^{\{1,(23)\}}$ and of $E_{3;0}^{\{1,(23)\}}$ in the pomeron and the odderon channel, respectively. The structure $Q_{4;0}$ vanishes in the quark–diquark limit. This is the result of a non-trivial cancellation of all terms of (66), making use of the identity (69). The pattern given by the impact factors in the small diquark limit is preserved by the small x evolution, in particular Q_4 vanishes.

In summary, we have verified that, in the quark–diquark limit, the baryon reduces to a dipole-like object with an asymmetric wave function, as it was expected. Conversely, our analysis shows that, outside the diquark limit, the baryon impact factor contains a new piece (related to $Q_{4;0}$), which accompanies the appearance of the third dipole-like term, $D_{2;0}^{\{2,3\}}$. A more detailed study of the question, to what extent the baryon wave functions actually favors a diquark state, should start from the Fourier transform of the overlap function, (95), which describes the distribution of the quarks in transverse coordinate space. Further work along these lines is in progress.

8 Discussion

In this paper we have investigated the high energy behavior of a baryonic state. We have studied the structure of a baryonic impact factor, its coupling to multi-gluon exchanges and the rapidity evolution of the t -channel gluon states. We found it convenient to follow very much the same approach, which has been developed and used for the high energy behavior of a virtual photon (or a heavy quarkonium state). For the scattering of such mesonic states, in the leading logarithmic approximation and in the large- N_c limit, the high energy behavior allows for the interpretation in terms of color dipoles, and one of the motivations of our investigation was the question to what extent this attractive physical picture can be used also for the scattering of baryonic states.

Compared to the quark–antiquark system created by the photon (or a heavy vector meson), the high energy scattering of baryonic systems consisting of three quarks shows similarities, but also striking differences. First, there is a component of the baryonic impact factor in which two of the three quarks interact with the target whereas the third one acts as a spectator. Here the two-quark subsystem behaves very much in the same way as the color singlet dipole of the quark–antiquark system. In particular, the rapidity evolution is the same as in the case of a virtual photon. This configuration, however, extends beyond the picture of a small “diquark state”: we have shown that, in the diquark limit, we recover the dipole picture. But the spectator quark is not necessarily linked (in transverse space) to one of the participating quarks, and our analysis includes also this more general configuration. Second, there is the piece of the baryon impact factor to which the C -odd three-gluon state (odderon) couples. Third, a new piece of the baryonic impact factor exists, which couples to a C -even three-gluon t -channel state, and there is a new vertex, which describes the transition from this three-gluon state to the four-gluon (two-pomeron) state. In the quark–antiquark case, there is no analogue of this contribution.

This third piece may actually be quite essential for the restauration of s -channel unitarity in baryon scattering and can therefore not be neglected. Namely, let us consider the scattering of a hypothetical heavy baryon on a large nuclear target; this represents the analogue of the Balitsky–

Kovchegov problem for the color dipole scattering. Based on our results, the baryon scattering amplitude \mathcal{B} can be written symbolically as a sum of the following pieces:

$$\mathcal{B} = \overbrace{D_2^{\{1,2\}} + D_2^{\{1,3\}} + D_2^{\{2,3\}}}^{C\text{-even}} + \overbrace{Q_4 + \mathcal{E}_3}^{C\text{-odd}}. \quad (104)$$

Here the first three terms, $D_2^{\{i,j\}}$, stand for the dipole-like contributions in which the baryon couples to the same two-point gluon correlator as the color dipole in the scattering of a virtual photon. The strength of this coupling, however, is only 1/2 of that for the photon dipole. The pieces Q_4 and \mathcal{E}_3 probe three-point gluon correlators: the C -even and C -odd ones respectively. As it was observed in the case of the color dipole in deep inelastic scattering, where only a single BFKL pomeron could couple to the dipole, we again see no indications of a direct two-pomeron coupling to the valence degrees of freedom of the baryon. If we assume that the two-gluon distribution probed by the first three terms in (104) is consistent with saturation of the black disc limit for color dipoles of the sizes given by the baryon geometry, then the T -matrices for each of the $D_2^{\{i,j\}}$ -components would tend to 1/2, and the total contribution of the dipole-like pieces to the baryon T -matrix would amount to 3/2. This would mean that s -channel unitarity can be maintained only if Q_4 and \mathcal{E}_3 give a combined contribution to the T -matrix smaller than $-1/2$. Thus, the three-reggeon states Q_4 and \mathcal{E}_3 seem to be essential to guarantee the s -channel unitarity. Interestingly enough, one might go even further and arrive at a quantitative prediction. If one postulates that the T -matrices, both for the color dipole and the baryon scattering at very large energies, saturate the unitarity limit, then one finds that in the black disc limit: (i) the C -odd three-point gluon correlator should vanish; this is due to the requirement that both proton and anti-proton scattering should reach the black disc limit, despite the fact that the amplitude \mathcal{E}_3 has opposite signs in these two cases; (ii) the C -even three-point correlator is strongly constrained: when coupled to the impact factor $Q_{4;0}$ it must lead to the scattering amplitude equal to $-1/2$. In the diquark limit, both $D_2^{\{2,3\}}$ and Q_4 vanish, and unitarization proceeds in the same way as in the dipole case.

We interpret these results as a strong indication that, in the context of baryon scattering, QCD reggeon field theory has to be extended beyond the theory of BFKL pomerons and their interactions. First, it is difficult to justify the large- N_c limit, which, in the scattering of virtual photon and mesonic states, allows one to reduce the evolution of BKP states consisting of $2n$ gluons to the propagation of n BFKL pomerons. Second, the three-gluon state (and its BKP evolution) seems to play an important rôle, not only in the odderon channel. As we have pointed out, this phenomenon is closely connected with the existence of the d reggeon, the even signature partner of the (odd signature) reggeized gluon.

On a deeper level one may speculate that there exists an intimate connection between the number of valence objects in the impact factor in the fundamental $SU(N_c)$

representation and the maximal number of reggeons in the BKP state that couple to the impact factor. For the quark–antiquark color dipole only the two-reggeon BFKL pomeron couples, and for the baryon containing three quarks we have both two- and three-reggeon states. We may conjecture that the number of the different BKP states that couple to the baryon in $SU(N_c)$ gauge theory is related to the number of Casimir operators of the gauge group. There exist two Casimir operators of the $SU(3)$ gauge group, and QCD reggeon field theory (whose basic degrees of freedom are the reggeized gluons) exhibits two ‘fundamental excitations’, which, in the leading-log approximation, are represented by the two-gluon BFKL pomeron and by the three-gluon odderon state. For a high energy $SU(N_c)$ baryon we expect that the impact factor, consisting of N_c quarks in the fundamental representation, would exhibit all the $2, 3, \dots, N_c$ gluon states, and this would be a hint that the number of fundamental glue excitations may be related to the $N_c - 1$ Casimir operators of $SU(N_c)$. It seems natural that the gauge group invariants should be mapped onto gauge invariant BKP states. The explicit connection, however, has not been yet established.

Turning to more practical and phenomenological applications, in this paper we have considered a baryonic state consisting of three massive quarks being in a proton-like configuration. One can view such a ‘heavy baryonium’ state as a convenient theoretical laboratory, very much in the same spirit as previous work on high energy QCD has made use of ‘heavy onium’ states. On the other hand, we feel that our results might also allow for immediate phenomenological applications. In particular, we have proposed a relativistic invariant model of the proton wave function, including the helicity structure and correlations between helicities and quark angular momenta. Both the model itself and the calculational technique applied may be useful in studies of polarized scattering of the proton and of the proton form factors. Another potential place of interest is the intermediate t region of proton–proton elastic scattering where, in the days of ISR experiments, a very simple three-gluon model had a striking phenomenological success [59]. It should also be quite interesting to study other applications of the model in the context of elastic pp and $p\bar{p}$ scattering and exclusive diffraction at RHIC, Tevatron and the LHC. Finally, we would like to view our study as a preparation for a QCD analysis of multiple scattering in pp collisions at the LHC.

Acknowledgements. We especially acknowledge the help of G.P. Vacca who contributed in the early stage of this work. We thank C. Ewerz, L. Lipatov, and M. Salvadore for interesting discussions, and A. Białas, S. Bondarenko, M. Diehl, Y. Kovchegov, E. Levin and R. Peschanski for useful comments. We thank the Galileo Galilei Institute in Florence for the support in the initial phase of this research project. L.M. gratefully acknowledges the support of the DFG grant SFB 676 and the grant of the Polish State Committee for Scientific Research No. 1 P03B 028 28.

Appendix A: Spinorial matrix elements

The calculations of the baryon wave functions and of the baryon scattering amplitudes are performed using the light-cone formalism summarized in [43].

Thus we employ the spinor basis defined by

$$\begin{Bmatrix} u_{\uparrow}(p) \\ u_{\downarrow}(p) \end{Bmatrix} = \frac{1}{\sqrt{p^+}}(p^+ + \hat{\beta}m + \hat{\alpha} \cdot \mathbf{p}) \times \begin{Bmatrix} \chi(\uparrow) \\ \chi(\downarrow) \end{Bmatrix} \quad (\text{A.1})$$

and

$$\begin{Bmatrix} v_{\uparrow}(p) \\ v_{\downarrow}(p) \end{Bmatrix} = \frac{1}{\sqrt{p^+}}(p^+ - \hat{\beta}m + \hat{\alpha} \cdot \mathbf{p}) \times \begin{Bmatrix} \chi(\downarrow) \\ \chi(\uparrow) \end{Bmatrix}, \quad (\text{A.2})$$

where

$$\chi(\uparrow) = \frac{1}{\sqrt{2}} \begin{pmatrix} 1 \\ 0 \\ 1 \\ 0 \end{pmatrix}, \quad \chi(\downarrow) = \frac{1}{\sqrt{2}} \begin{pmatrix} 0 \\ 1 \\ 0 \\ -1 \end{pmatrix} \quad (\text{A.3})$$

in the Dirac representation, and the Dirac matrices $\hat{\beta}$ and $\hat{\alpha}$ are related to the γ -matrices through $\hat{\beta} = \gamma^0$ and $\hat{\alpha}^s = \gamma^0 \gamma^s$; m is the mass of a fermion (or an anti-fermion). In the infinite momentum frame, when $p^+ \rightarrow \infty$ these spinors tend to the helicity eigenstates, $u_{\uparrow\downarrow}(p) \rightarrow u_{\pm}(p)$, $v_{\uparrow\downarrow}(p) \rightarrow v_{\pm}(p)$.

In the calculation of the baryon \rightarrow quarks transition amplitudes it is sufficient to employ the spinor matrix elements given in Table 1. Note that we consider a general case in which the masses of the spinors u (or v) and u' are given by m and m' , respectively.

As an example, we apply the formulae of Table 1 to evaluate

$$\begin{aligned} & \frac{[\bar{d}_{\lambda_3}(p_3)\gamma_{\mu}w_{\lambda}(P)] \cdot [\bar{u}_{\lambda_1}(p_1)\gamma^{\mu}v_{\lambda_2}(p_2)]}{\sqrt{P^+p_1^+p_2^+p_3^+}} \\ &= \frac{1}{2} \frac{[\bar{d}_{\lambda}(p_3)\gamma^+w_{\lambda}(P)] \cdot [\bar{u}_{\lambda_1}(p_1)\gamma^-v_{\lambda_2}(p_2)]}{\sqrt{P^+p_1^+p_2^+p_3^+}} \\ &+ \frac{1}{2} \frac{[\bar{d}_{\lambda}(p_3)\gamma^-w_{\lambda}(P)] \cdot [\bar{u}_{\lambda_1}(p_1)\gamma^+v_{\lambda_2}(p_2)]}{\sqrt{P^+p_1^+p_2^+p_3^+}} \\ &- \frac{[\bar{d}_{\lambda}(p_3)\gamma_{\perp}^s w_{\lambda}(P)] \cdot [\bar{u}_{\lambda_1}(p_1)\gamma_{\perp}^s v_{\lambda_2}(p_2)]}{\sqrt{P^+p_1^+p_2^+p_3^+}} \end{aligned} \quad (\text{A.4})$$

for $\lambda = \lambda_1 = -\lambda_2 = \lambda_3 = +1$. The prefactors $1/2$, $1/2$ and -1 on the r.h.s. are the only non-vanishing elements of the covariant metric tensor $g_{\mu\nu}$ in the light-cone coordinates. In the calculations we find it useful to make use of the following identities for transverse complex vectors $\boldsymbol{\eta}_{\pm}$: $\boldsymbol{\eta}_{+}^* = \boldsymbol{\eta}_{-}$, $\boldsymbol{\eta}_{\pm}^2 = 0$, $\boldsymbol{\eta}_{\pm} \cdot \boldsymbol{\eta}_{\mp} = |\boldsymbol{\eta}_{\pm}|^2 = 2$. Thus, assuming that the light quark masses vanish, we

Table 1. Matrix elements of Dirac spinors in the Brodsky–Lepage basis

Matrix element	$\lambda \rightarrow \lambda'$	$\lambda \rightarrow \lambda'$
$\bar{u}'_{\lambda'}(p) \dots u_{\lambda}(q)$	$\uparrow \rightarrow \uparrow$ $\downarrow \rightarrow \downarrow$	$\uparrow \rightarrow \downarrow$ $\downarrow \rightarrow \uparrow$
$\frac{\bar{u}'(p)}{\sqrt{p^+}} \gamma^+ \frac{u(q)}{\sqrt{q^+}}$	2	0
$\frac{\bar{u}'(p)}{\sqrt{p^+}} \gamma^- \frac{u(q)}{\sqrt{q^+}}$	$\frac{2}{p^+ q^+} [(\mathbf{p} \cdot \boldsymbol{\eta}_{\mp})(\mathbf{q} \cdot \boldsymbol{\eta}_{\pm}) + mm']$	$\mp \frac{2}{p^+ q^+} (m \mathbf{p} \cdot \boldsymbol{\eta}_{\pm} - m' \mathbf{q} \cdot \boldsymbol{\eta}_{\pm})$
$\frac{\bar{u}'(p)}{\sqrt{p^+}} \gamma^{\perp} \frac{u(q)}{\sqrt{q^+}}$	$\eta_{\pm}^s \frac{\mathbf{p} \cdot \boldsymbol{\eta}_{\mp}}{p^+} + \eta_{\mp}^s \frac{\mathbf{q} \cdot \boldsymbol{\eta}_{\pm}}{q^+}$	$\pm \eta_{\pm}^s \left(\frac{m'}{p^+} - \frac{m}{q^+} \right)$
Matrix element	$\lambda \rightarrow \lambda'$	$\lambda \rightarrow \lambda'$
$\bar{v}'_{\lambda'}(p) \dots u_{\lambda}(q)$	$\uparrow \rightarrow \uparrow$ $\downarrow \rightarrow \downarrow$	$\uparrow \rightarrow \downarrow$ $\downarrow \rightarrow \uparrow$
$\frac{\bar{v}'(p)}{\sqrt{p^+}} \gamma^+ \frac{u(q)}{\sqrt{q^+}}$	0	2
$\frac{\bar{v}'(p)}{\sqrt{p^+}} \gamma^- \frac{u(q)}{\sqrt{q^+}}$	$\mp \frac{2}{p^+ q^+} (m \mathbf{p} \cdot \boldsymbol{\eta}_{\pm} + m' \mathbf{q} \cdot \boldsymbol{\eta}_{\pm})$	$\frac{2}{p^+ q^+} [(\mathbf{p} \cdot \boldsymbol{\eta}_{\mp})(\mathbf{q} \cdot \boldsymbol{\eta}_{\pm}) - mm']$
$\frac{\bar{v}'(p)}{\sqrt{p^+}} \gamma^{\perp} \frac{u(q)}{\sqrt{q^+}}$	$\mp \eta_{\pm}^s \left(\frac{m'}{p^+} + \frac{m}{q^+} \right)$	$\eta_{\pm}^s \frac{\mathbf{p} \cdot \boldsymbol{\eta}_{\mp}}{p^+} + \eta_{\mp}^s \frac{\mathbf{q} \cdot \boldsymbol{\eta}_{\pm}}{q^+}$

obtain

$$\begin{aligned}
& \frac{[\bar{d}_{\lambda_3}(p_3) \gamma_{\mu} w_{\lambda}(P)] \cdot [\bar{v}_{\lambda_2}(p_2) \gamma^{\mu} u_{\lambda_1}(p_1)]^*}{\sqrt{P^+ p_1^+ p_2^+ p_3^+}} \\
&= \frac{2[(\mathbf{p}_2 \cdot \boldsymbol{\eta}_{-})(\mathbf{p}_1 \cdot \boldsymbol{\eta}_{+})]^*}{p_1^+ p_2^+} + \frac{2(\mathbf{p}_3 \cdot \boldsymbol{\eta}_{-})(\mathbf{P} \cdot \boldsymbol{\eta}_{+})}{P^+ p_3^+} \\
&\quad - \frac{2(\mathbf{p}_3 \cdot \boldsymbol{\eta}_{-})(\mathbf{p}_2 \cdot \boldsymbol{\eta}_{-})^*}{p_2^+ p_3^+} - \frac{2(\mathbf{P} \cdot \boldsymbol{\eta}_{+})(\mathbf{p}_1 \cdot \boldsymbol{\eta}_{+})^*}{P^+ p_1^+} \\
&= 2 \left[\frac{\mathbf{p}_2 \cdot \boldsymbol{\eta}_{+}}{p_2^+} - \frac{\mathbf{P} \cdot \boldsymbol{\eta}_{+}}{P^+} \right] \left[\frac{\mathbf{p}_1 \cdot \boldsymbol{\eta}_{-}}{p_1^+} - \frac{\mathbf{p}_3 \cdot \boldsymbol{\eta}_{-}}{p_3^+} \right]. \quad (\text{A.5})
\end{aligned}$$

Using an identity³ $\bar{d}_{\lambda_3}(p_3) \gamma_5 = \lambda_3 \bar{d}_{\lambda_3}(p_3)$, and (10), one obtains one of the matrix elements described by (21). The matrix elements for all remaining choices of helicities can be derived in the same way.

Appendix B: A reduction formula for spinors in the high energy limit

We shall prove the following identity for massive Dirac spinors:

$$\bar{u}(p) \hat{q}(\hat{p} + m + \hat{k}) = 2p \cdot q \bar{u}(p + k) + \dots, \quad (\text{B.1})$$

which holds, at the leading accuracy in $s \simeq 2p \cdot q$, in the high energy limit: $s \gg q^2, k^2, m^2, p \cdot k, q \cdot k$ etc., and for $k_{\perp} \gg k^+, k^-$. This identity is a useful tool for deriving quark scattering amplitudes by multi-gluon couplings in the eikonal approximation. Using the spinor equation of

motion, $\bar{u}(p)(\hat{p} - m) = 0$, we get

$$\bar{u}(p) \hat{q}(\hat{p} + m + \hat{k}) = \bar{u}(p)(2p \cdot q + \hat{q} \hat{k}) \simeq s \bar{u}(p) \left(1 + \frac{1}{2s} [\hat{q}, \hat{k}] \right), \quad (\text{B.2})$$

where we used the fact that the anticommutator $\{\hat{q}, \hat{k}\} = 2k \cdot q \ll s$. Furthermore, using the light-cone variables, as defined in Sect. 3, we have

$$[\hat{q}, \hat{k}] = -2i \hat{\sigma}_{\alpha\beta} q^{\alpha} k^{\beta} \simeq -2i \hat{\sigma}_{-r} q^{-} k_{\perp}^r, \quad (\text{B.3})$$

where r is the Lorentz index of the transverse coordinates. Thus one obtains

$$\bar{u}(p) \hat{q}(\hat{p} + m + \hat{k}) \simeq s \bar{u}(p) \left(1 - \frac{i \hat{\sigma}_{-r} k_{\perp}^r}{p^+} \right). \quad (\text{B.4})$$

The matrices $\hat{\sigma}^{\alpha\beta}$ are proportional to the generators of the Lorentz transformations of the Dirac spinors:

$$\begin{aligned}
& \exp\left(-\frac{i}{4} \sigma_{\alpha\beta} \omega^{\alpha\beta}\right) u(p) = u(\Lambda(\omega)p), \\
& \bar{u}(p) \exp\left(\frac{i}{4} \sigma_{\alpha\beta} \omega^{\alpha\beta}\right) = \bar{u}(\Lambda(\omega)p), \quad (\text{B.5})
\end{aligned}$$

where

$$(\Lambda(\omega)p)^{\mu} = [\Lambda(\omega)]^{\mu}_{\nu} p^{\nu}, \quad \Lambda(\omega) = \exp\left(\frac{1}{2} \omega^{\alpha\beta} L_{\alpha\beta}\right), \quad (\text{B.6})$$

and the generators of Lorentz transformations in the vector representation read

$$[L_{\alpha\beta}]^{\mu}_{\nu} = g^{\mu}_{\alpha} g_{\nu\beta} - g^{\mu}_{\beta} g_{\nu\alpha}. \quad (\text{B.7})$$

Since the parameter multiplying $\hat{\sigma}_{-r}$ in (B.4) is small, $\beta^r = k_{\perp}^r/p^+ \ll 1$, one may write

$$\begin{aligned}
& \bar{u}(p) (1 - i \hat{\sigma}_{-r} \beta^r) = \bar{u}(p) [\exp(-i \hat{\sigma}_{0r} \beta^r/2) \exp(i \hat{\sigma}_{3r} \beta^r/2)] \\
& \quad + O(\beta^2), \quad (\text{B.8})
\end{aligned}$$

³ For a non-zero quark mass m , this relation holds approximately in the large energy limit: $\bar{d}_{\lambda_3}(p_3) \gamma_5 = \lambda_3 \bar{d}_{\lambda_3}(p_3) + O(m/p_3^+)$.

where we used the identity $\gamma_- = \frac{1}{2}(\gamma_0 - \gamma_3)$. This equation corresponds to two subsequent infinitesimal Lorentz transformations acting on $\bar{u}(p)$ with the parameters $\omega_1^{r0} = -\omega_1^{0r} = \beta^r$ and $\omega_2^{3r} = -\omega_2^{r3} = \beta^r$ (and all other components $\omega_{1,2}^{\alpha\beta} = 0$). This is an infinitesimal boost along the transverse direction β , and an infinitesimal rotation in the plane spanned by the transverse vector β around the z -axis. Using (B.5) one sees that, in leading order in β^r , the boost transforms p in the following way: $p^0 \rightarrow p^0$, $\mathbf{p} \rightarrow \mathbf{p} + p^0 \beta$, $p^3 \rightarrow p^3$, and the rotation acts as $p^0 \rightarrow p^0$, $\mathbf{p} \rightarrow \mathbf{p} + p^3 \beta$, $p^3 \rightarrow p^3$. Thus one obtains

$$\bar{u}(p)(1 - i\hat{\sigma}_{-r}\beta^r) = \bar{u}(p') + O(\beta^2), \quad (\text{B.9})$$

with $p' = (p^0, \mathbf{p} + \beta p^+, p^3)$. This proves (B.1). The equation for multiple eikonal couplings, (15), follows immediately from (B.1), after all spinor contractions, $\hat{q}(\hat{p} - \hat{k}_1 - \dots - \hat{k}_i + m)\hat{q} \simeq 2p \cdot \hat{q}\hat{q}$, are executed.

References

1. L.N. Lipatov, Sov. J. Nucl. Phys. **23**, 338 (1976)
2. L.N. Lipatov, Yad. Fiz. **23**, 642 (1976)
3. E.A. Kuraev, L.N. Lipatov, V.S. Fadin, Sov. Phys. JETP **45**, 199 (1977)
4. E.A. Kuraev, L.N. Lipatov, V.S. Fadin, Zh. Eksp. Teor. Fiz. **72**, 377 (1977)
5. I.I. Balitsky, L.N. Lipatov, Sov. J. Nucl. Phys. **28**, 822 (1978)
6. I.I. Balitsky, L.N. Lipatov, Yad. Fiz. **28**, 1597 (1978)
7. L.N. Lipatov, Phys. Rep. **286**, 131 (1997)
8. V.S. Fadin, L.N. Lipatov, Phys. Lett. B **429**, 127 (1998)
9. M. Ciafaloni, G. Camici, Phys. Lett. B **430**, 349 (1998)
10. V.S. Fadin, R. Fiore, Phys. Lett. B **610**, 61 (2005)
11. V.S. Fadin, R. Fiore, Phys. Lett. B **621**, 61 (2005) [Erratum]
12. V.S. Fadin, R. Fiore, Phys. Rev. D **72**, 014018 (2005)
13. I. Balitsky, Nucl. Phys. B **463**, 99 (1996)
14. Y.V. Kovchegov, Phys. Rev. D **60**, 034008 (1999)
15. Y.V. Kovchegov, Phys. Rev. D **61**, 074018 (2000)
16. J. Bartels, L.N. Lipatov, G.P. Vacca, Nucl. Phys. B **706**, 391 (2005)
17. N.N. Nikolaev, B.G. Zakharov, Z. Phys. C **49**, 607 (1991)
18. N.N. Nikolaev, B.G. Zakharov, Z. Phys. C **53**, 331 (1992)
19. A.H. Mueller, Nucl. Phys. B **415**, 373 (1994)
20. J. Bartels, Z. Phys. C **60**, 471 (1993)
21. J. Jalilian-Marian, A. Kovner, H. Weigert, Phys. Rev. D **59**, 014015 (1999)
22. J. Jalilian-Marian, A. Kovner, A. Leonidov, H. Weigert, Phys. Rev. D **59**, 014014 (1999)
23. E. Iancu, A. Leonidov, L.D. McLerran, Nucl. Phys. A **692**, 583 (2001)
24. E. Iancu, A. Leonidov, L.D. McLerran, Phys. Lett. B **510**, 133 (2001)
25. E. Iancu, L.D. McLerran, Phys. Lett. B **510**, 145 (2001)
26. E. Ferreiro, E. Iancu, A. Leonidov, L. McLerran, Nucl. Phys. A **703**, 489 (2002)
27. M. Praszalowicz, A. Rostworowski, Acta Phys. Pol. B **29**, 745 (1998)
28. B.L. Ioffe, Nucl. Phys. B **188**, 317 (1981)
29. B.L. Ioffe, Nucl. Phys. B **191**, 591 (1981) [Erratum]
30. V.M. Braun, A. Lenz, M. Wittmann, Phys. Rev. D **73**, 094019 (2006)
31. J. Bartels, M. Wüsthoff, Z. Phys. C **66**, 157 (1995)
32. J. Bartels, C. Ewerz, JHEP **9909**, 026 (1999)
33. S. Braunewell, C. Ewerz, Nucl. Phys. A **760**, 141 (2005)
34. J. Bartels, Nucl. Phys. B **151**, 293 (1979)
35. J. Bartels, Nucl. Phys. B **175**, 365 (1980)
36. J. Kwieciński, M. Praszalowicz, Phys. Lett. B **94**, 413 (1980)
37. M.A. Shifman, A.I. Vainshtein, V.I. Zakharov, Nucl. Phys. B **147**, 385 (1979)
38. I.I. Balitsky, L.N. Lipatov, JETP Lett. **30**, 355 (1979)
39. I.I. Balitsky, L.N. Lipatov, Pisma. Zh. Eksp. Teor. Fiz. **30**, 383 (1979)
40. A. Ivanov, R. Kirschner, Eur. Phys. J. C **29**, 353 (2003)
41. V. Braun, R.J. Fries, N. Mahnke, E. Stein, Nucl. Phys. B **589**, 381 (2000)
42. V. Braun, R.J. Fries, N. Mahnke, E. Stein, Nucl. Phys. B **607**, 433 (2001) [Erratum]
43. G.P. Lepage, S.J. Brodsky, Phys. Rev. D **22**, 2157 (1980)
44. S.J. Brodsky, T. Huang, G.P. Lepage, in Particles and Fields 2, Proc. of the Banff Summer Institute, Banff, Alberta, 1981, ed. by A.Z. Capri, A.N. Kamal (Plenum, New York, 1981), p. 143
45. J. Bolz, P. Kroll, Z. Phys. A **356**, 327 (1996)
46. M. Diehl, Phys. Rep. **388**, 41 (2003)
47. Y.V. Kovchegov, Phys. Rev. D **64**, 114016 (2001)
48. Y.V. Kovchegov, Phys. Rev. D **68**, 039901 (2003) [Erratum]
49. M. Fukugita, J. Kwieciński, Phys. Lett. B **83**, 1 (1979)
50. J. Czyżewski, J. Kwieciński, L. Motyka, M. Sadzikowski, Phys. Lett. B **398**, 400 (1997)
51. J. Czyżewski, J. Kwieciński, L. Motyka, M. Sadzikowski, Phys. Lett. B **411**, 402 (1997) [Erratum]
52. Y. Hatta, E. Iancu, K. Itakura, L. McLerran, Nucl. Phys. A **760**, 172 (2005)
53. M. Salvadore, PhD thesis (Bologna University, 2006)
54. J. Bartels, M. Salvadore, G.P. Vacca, arXiv:0802.2702 [hep-ph]
55. M.A. Braun, G.P. Vacca, Eur. Phys. J. C **6**, 147 (1999)
56. J. Bartels, L.N. Lipatov, G.P. Vacca, Phys. Lett. B **477**, 178 (2000)
57. J. Wosiek, R.A. Janik, Phys. Rev. Lett. **79**, 2935 (1997)
58. R.A. Janik, J. Wosiek, Phys. Rev. Lett. **82**, 1092 (1999)
59. P.V. Landshoff, Phys. Rev. D **10**, 1024 (1974)